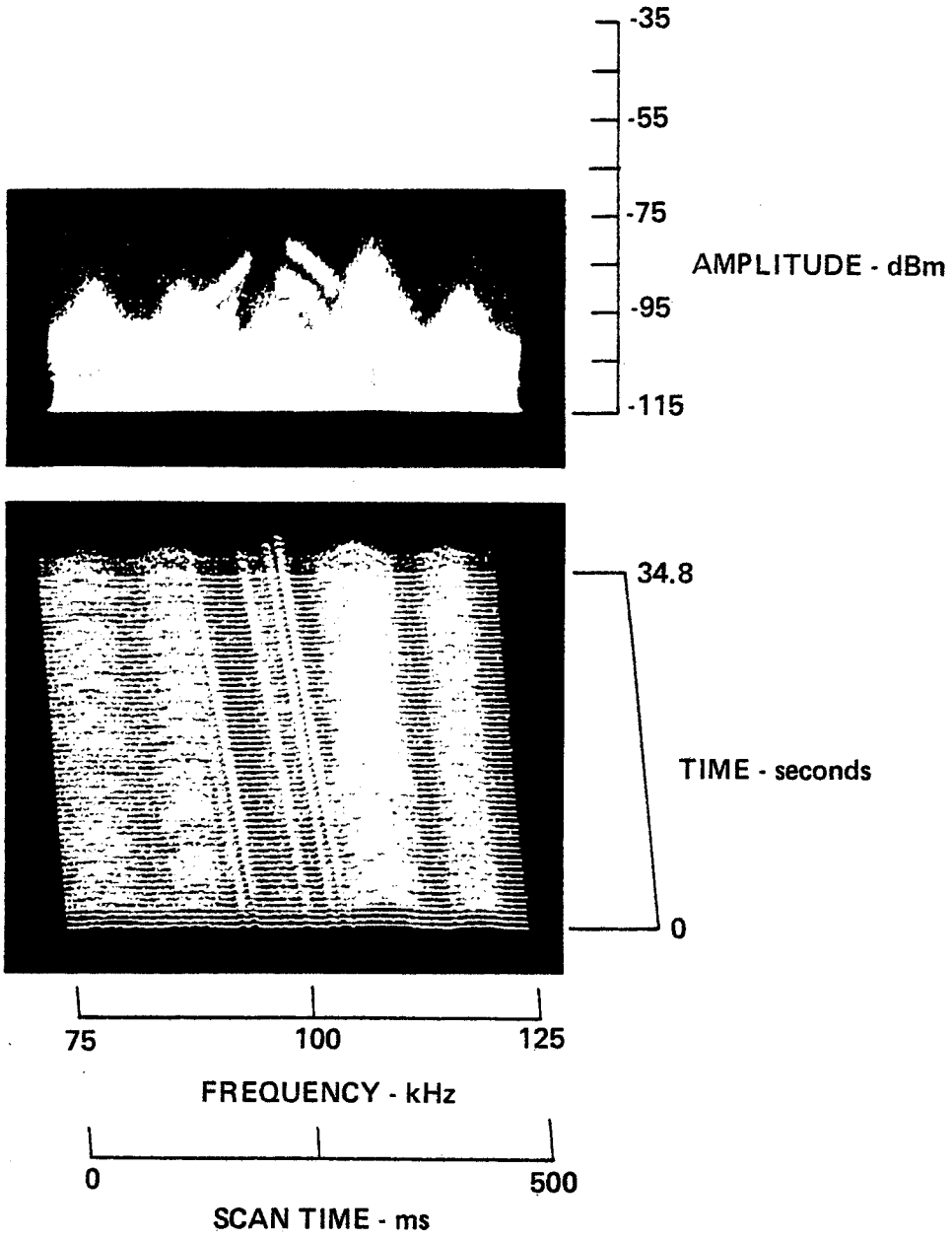

1-25-79, 0752, 110-041
HP140, Whip, F100, W50, IF3, ST 500, A -20/0/+15/NF

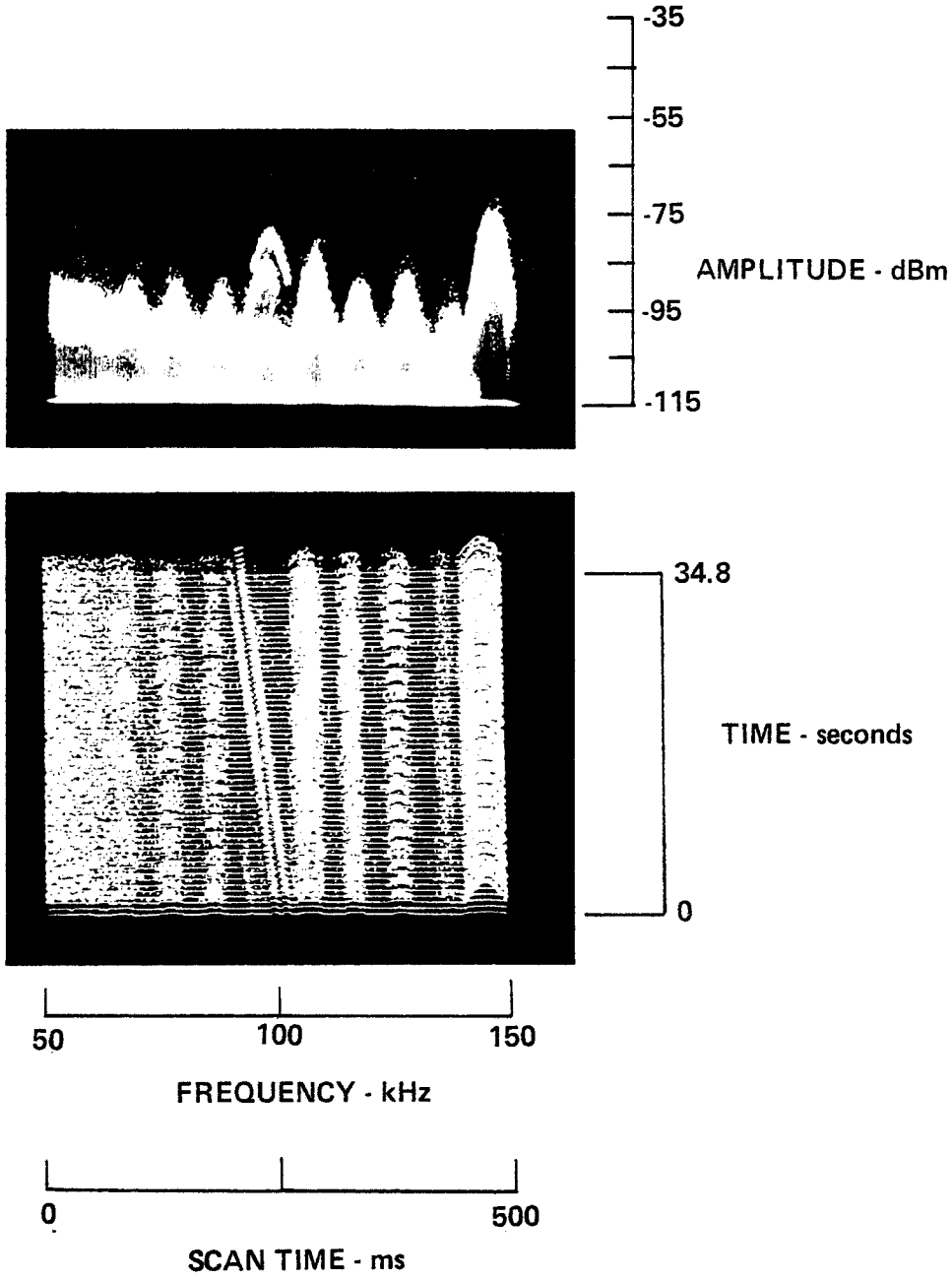

1-25-79, 0757, 110-041
HP140, Whip, F100, W100, IF3, ST 500, A -20/0/+15/NF

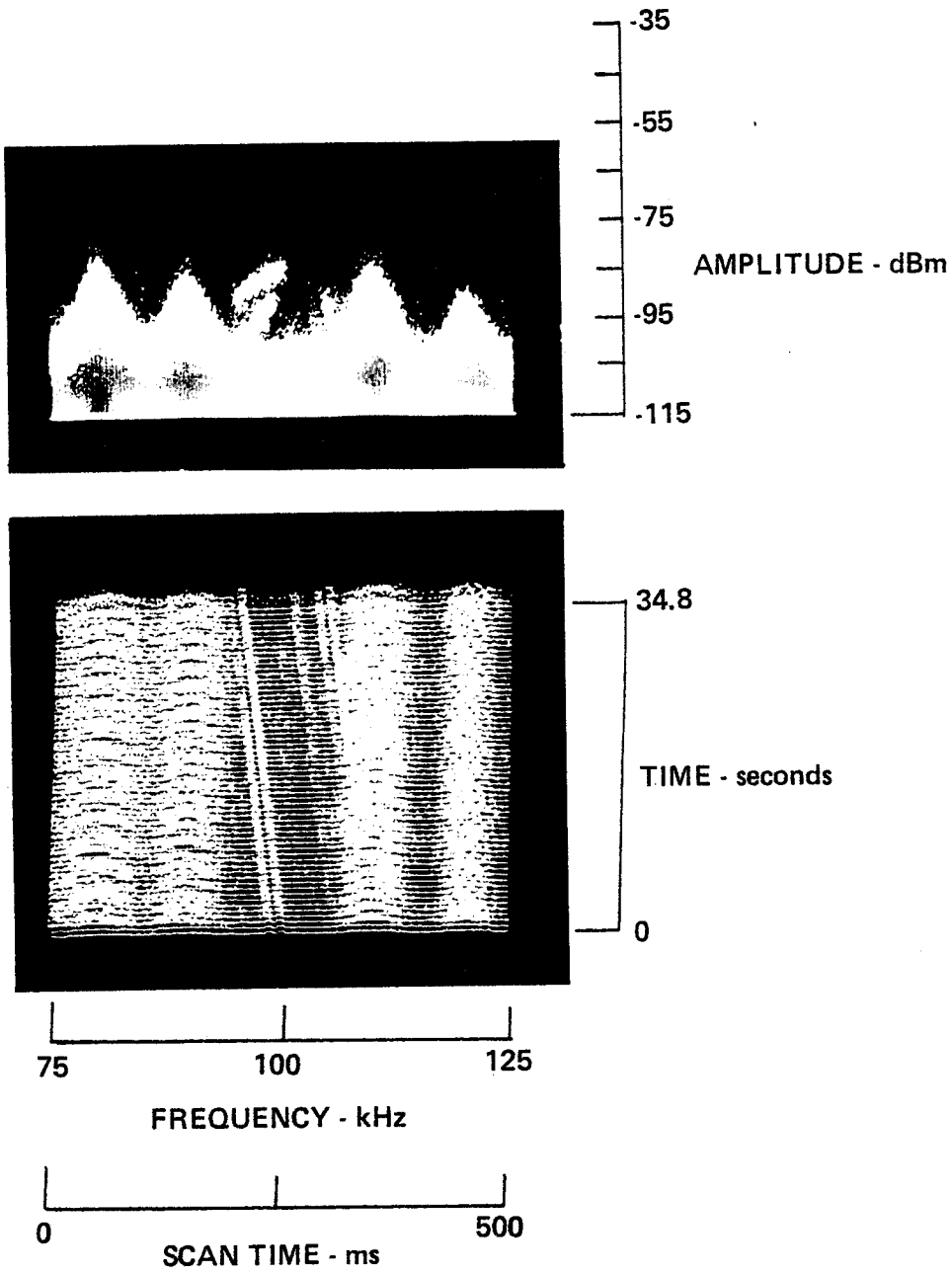

1-25-79, 0803, 110-042
HP140, Whip, F100, W50, IF3, ST 500, A -20/0/+15/NF

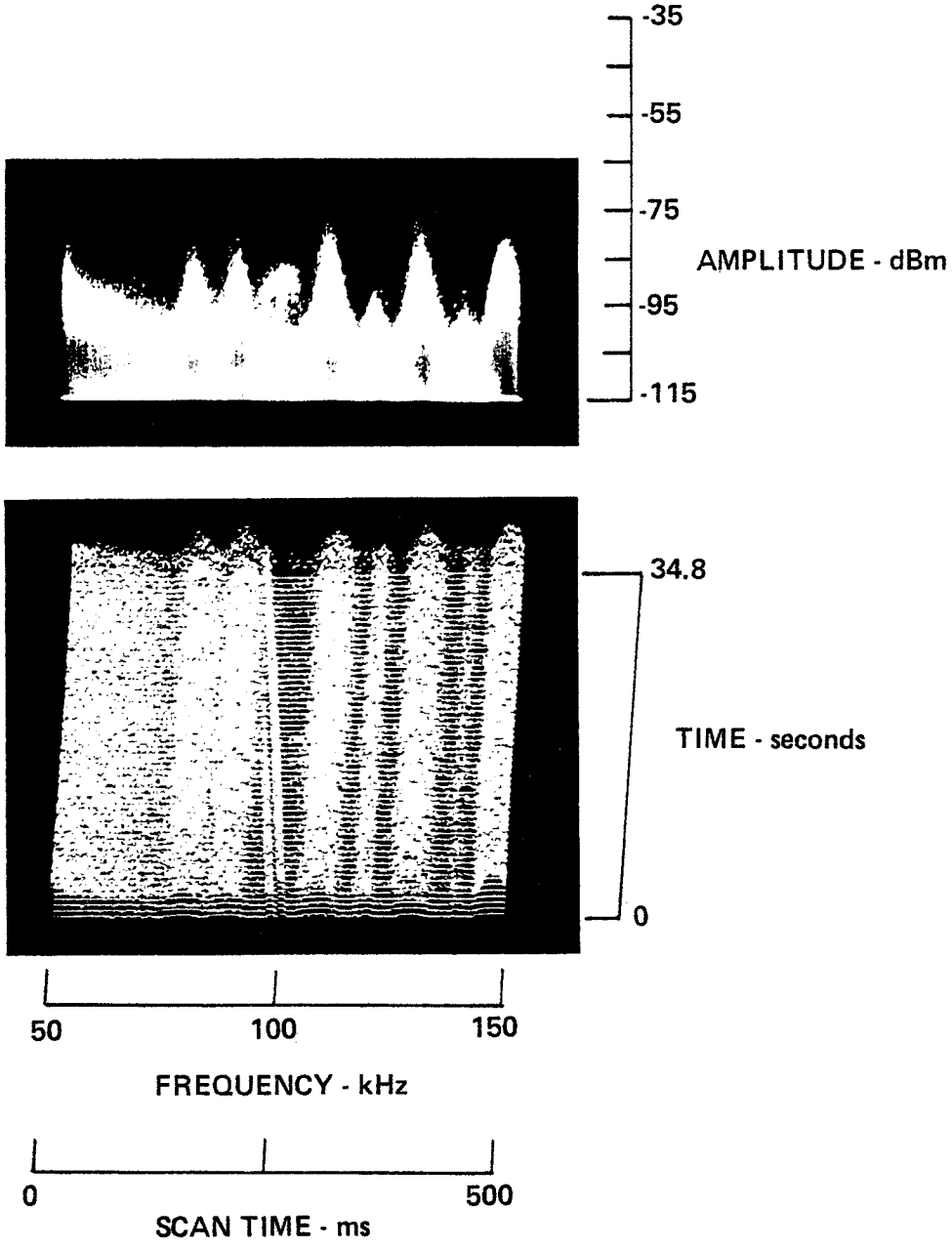

1-25-79, 0810, 110-042
HP140, Whip, F100, W100, IF3, ST 500, A -20/0/+15

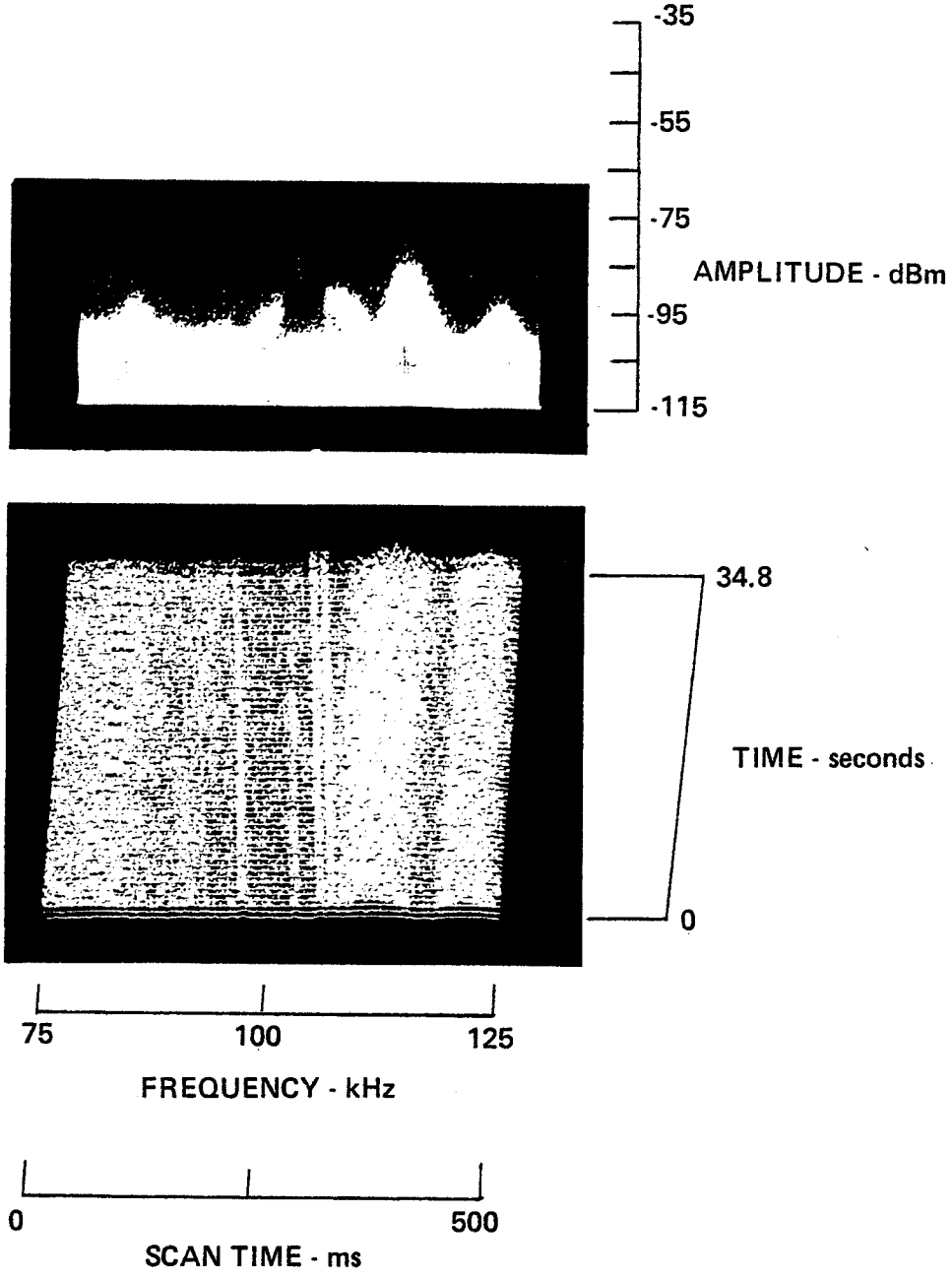

1-25-79, 0817, 110-044
HP140, Whip, F100, W50, IF3, ST 500, A -20/0/+15/NF

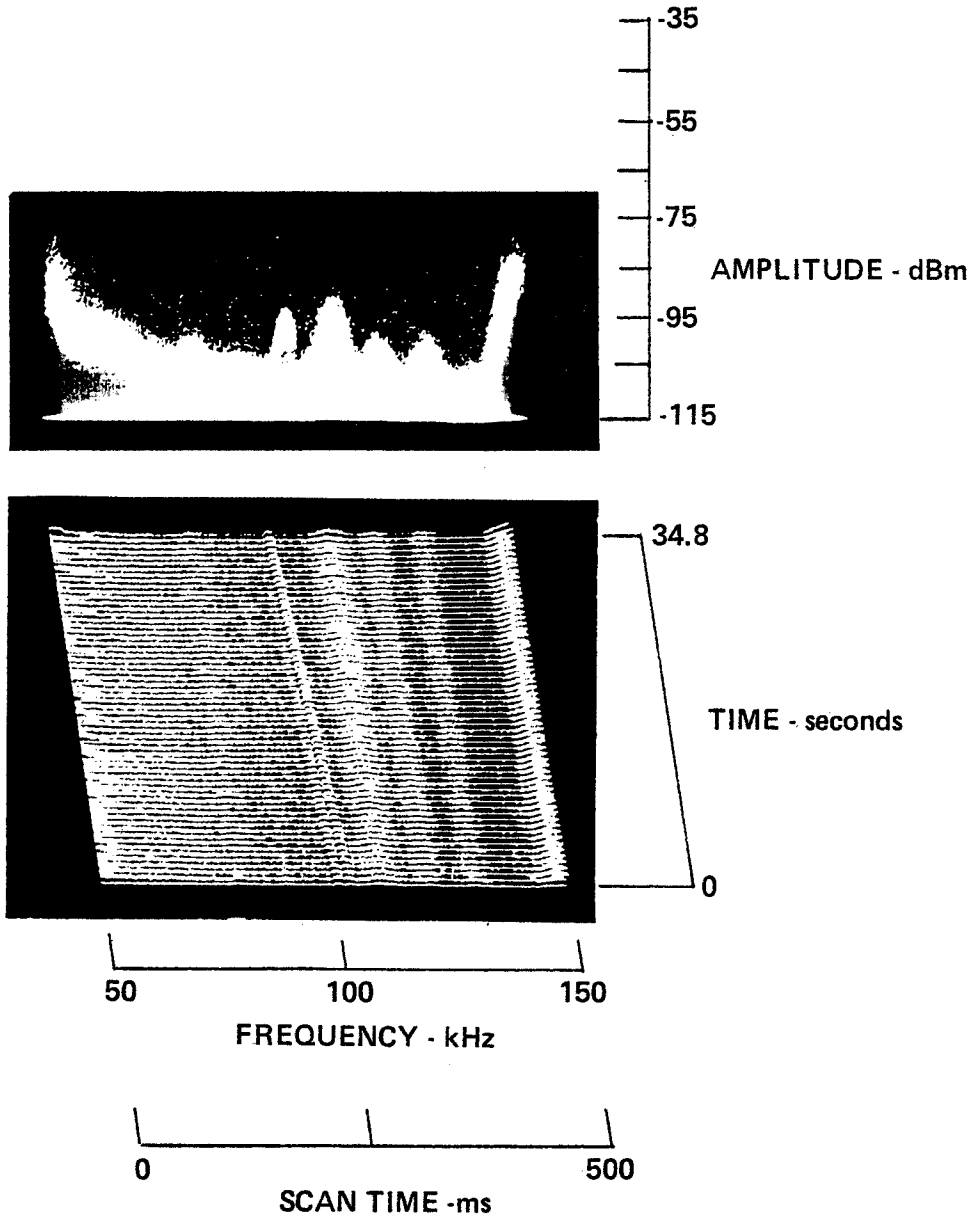

1-25-79, 0823, 110-044
HP140, Whip, F100, W100, IF3, ST 500, A -20/0/+15/NF

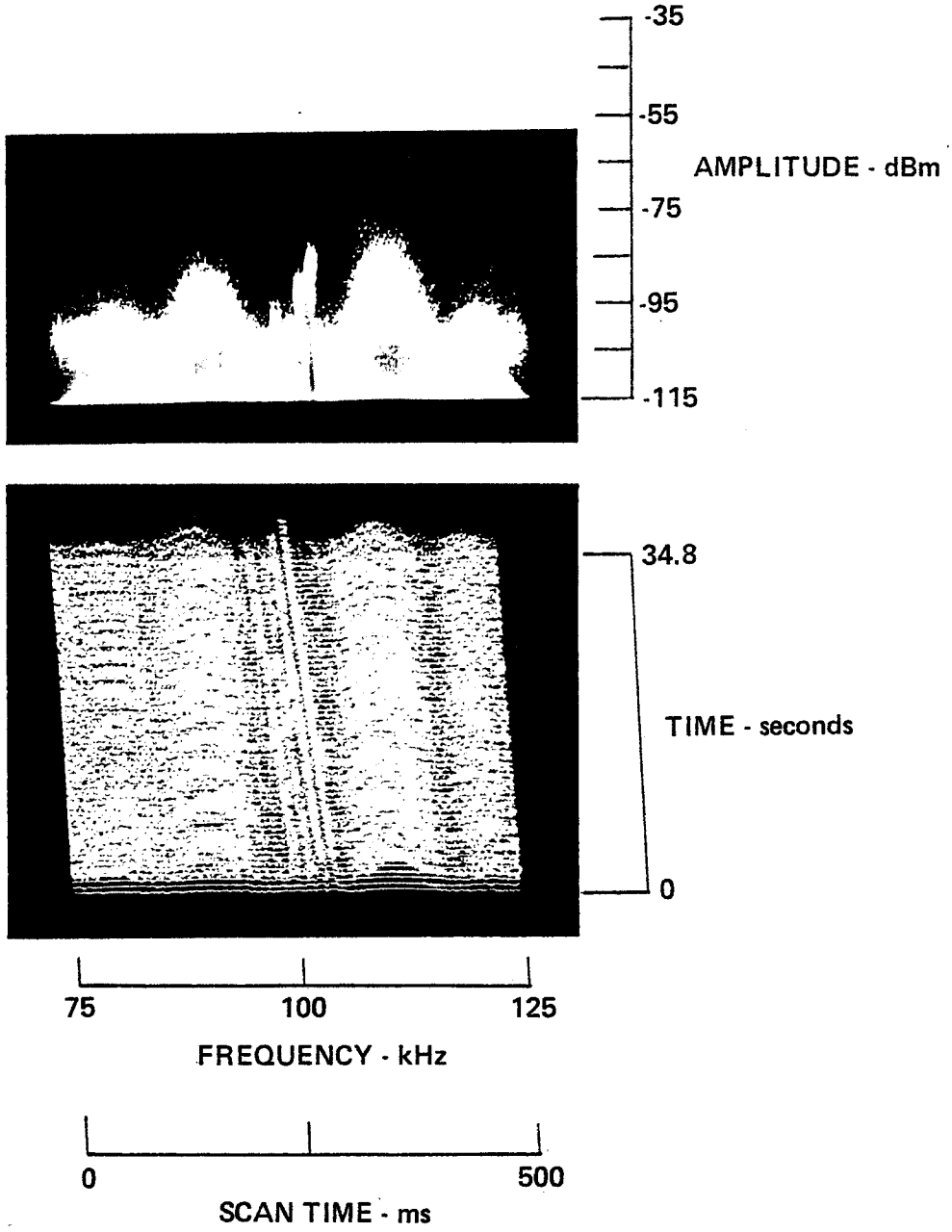

1-25-79, 0833, 110-045
HP140, Whip, F100, W50, IF3, ST 500, A -20/0/+15/NF

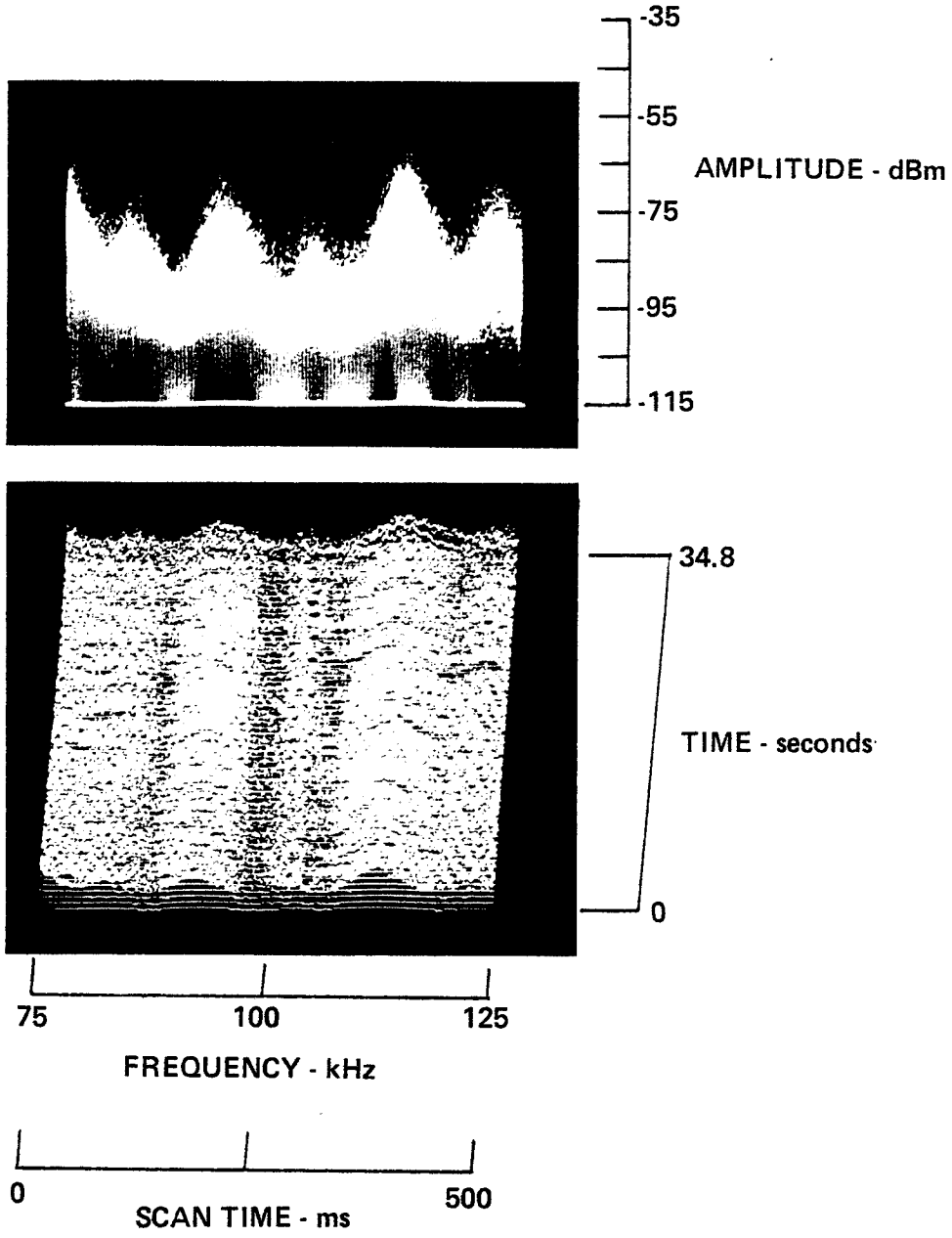

1-25-79, 0846, 110-046
HP140, Whip, F100, W50, IF3, ST500, A -20/0/+15/NF

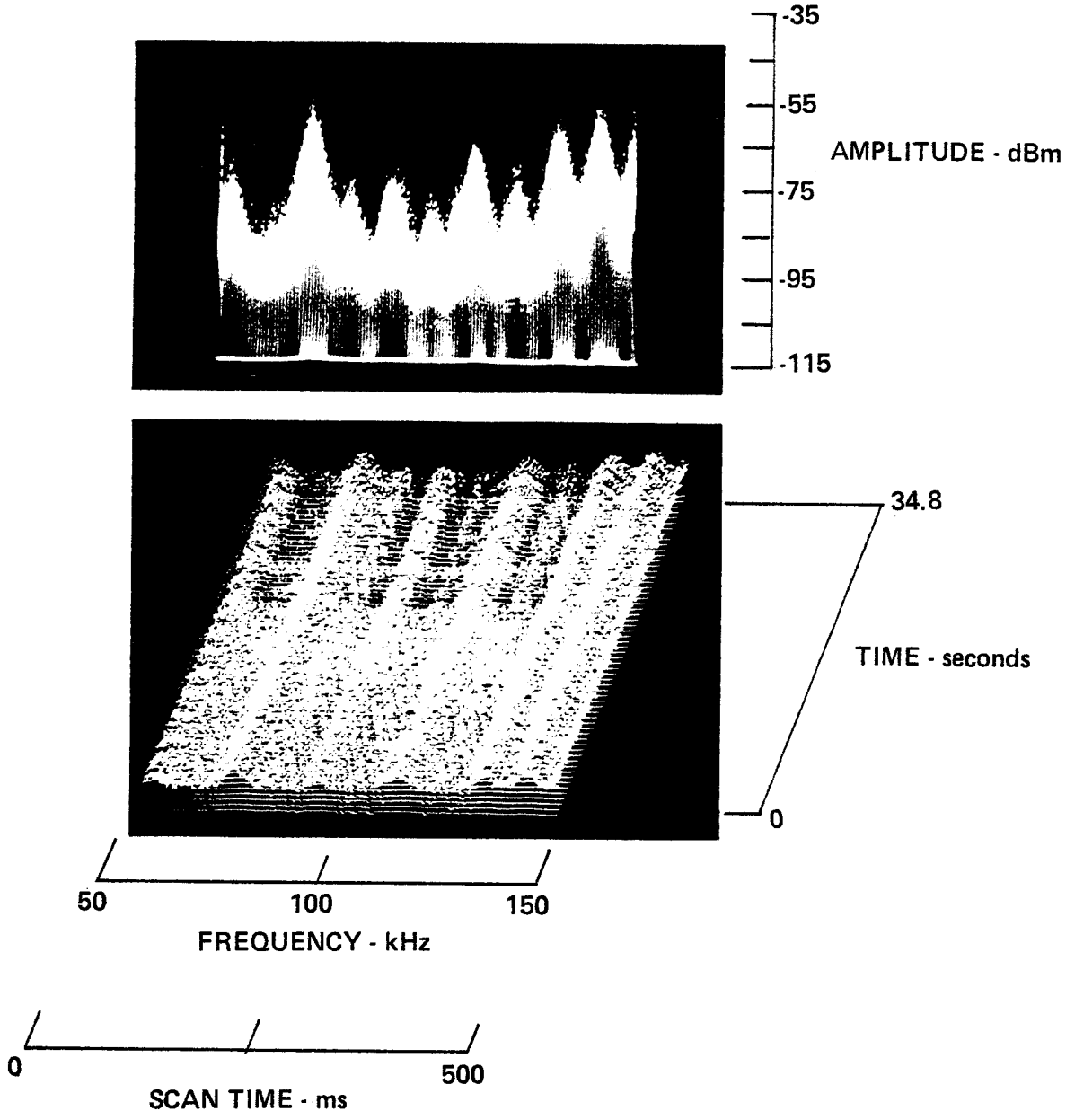

1-25-79, 0853, 110-046,
HP140, Whip, F100, W100, IF3, ST 500, A -20/0/+15/NF

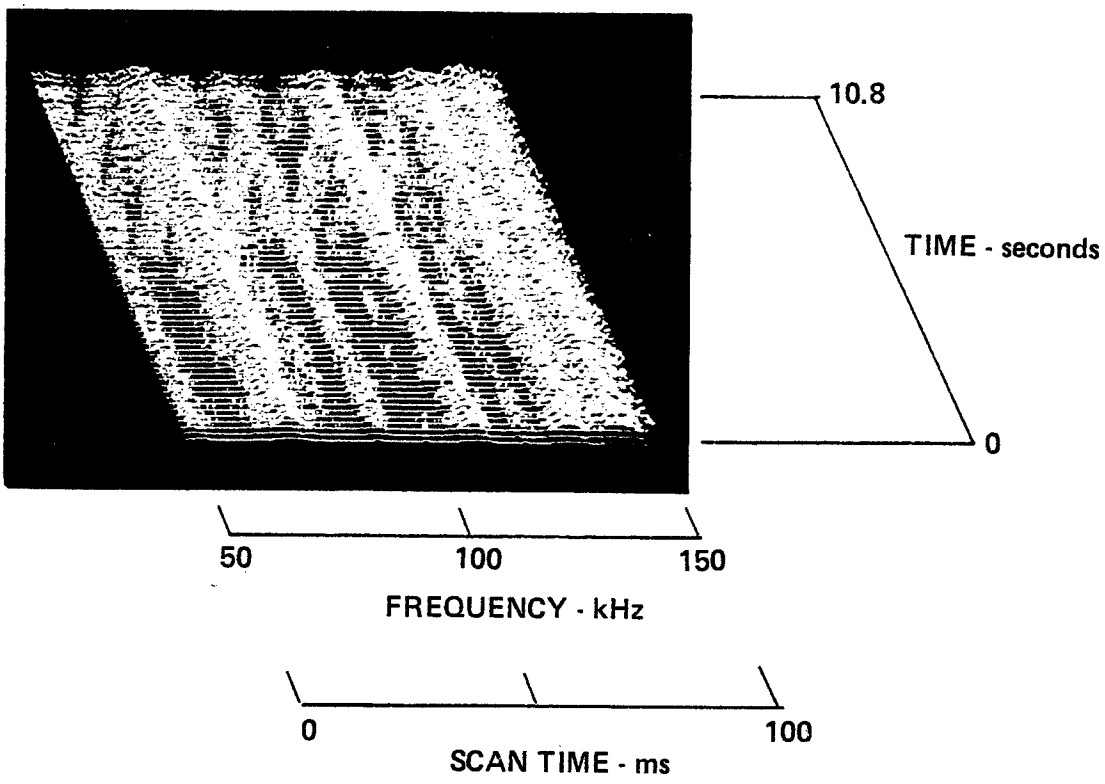

1-25-79, 0851, 110-046
HP140, Whip, F100, W100, IF3, ST 100, A -20/0/+15/NF

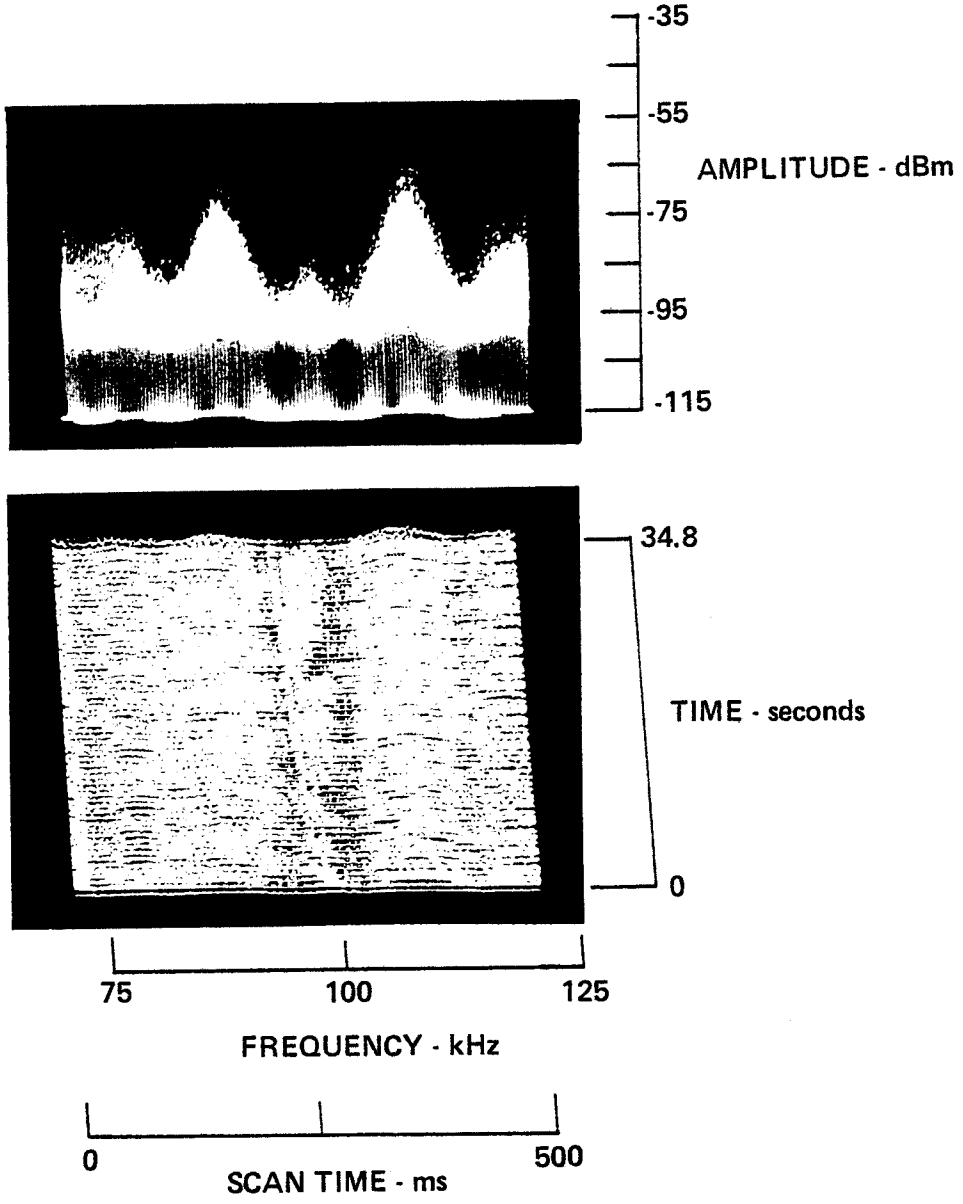

1-25-79, 0904, 110-047
HP140, Whip, F100, W50, IF3, ST 500, A -20/0/+15/NF

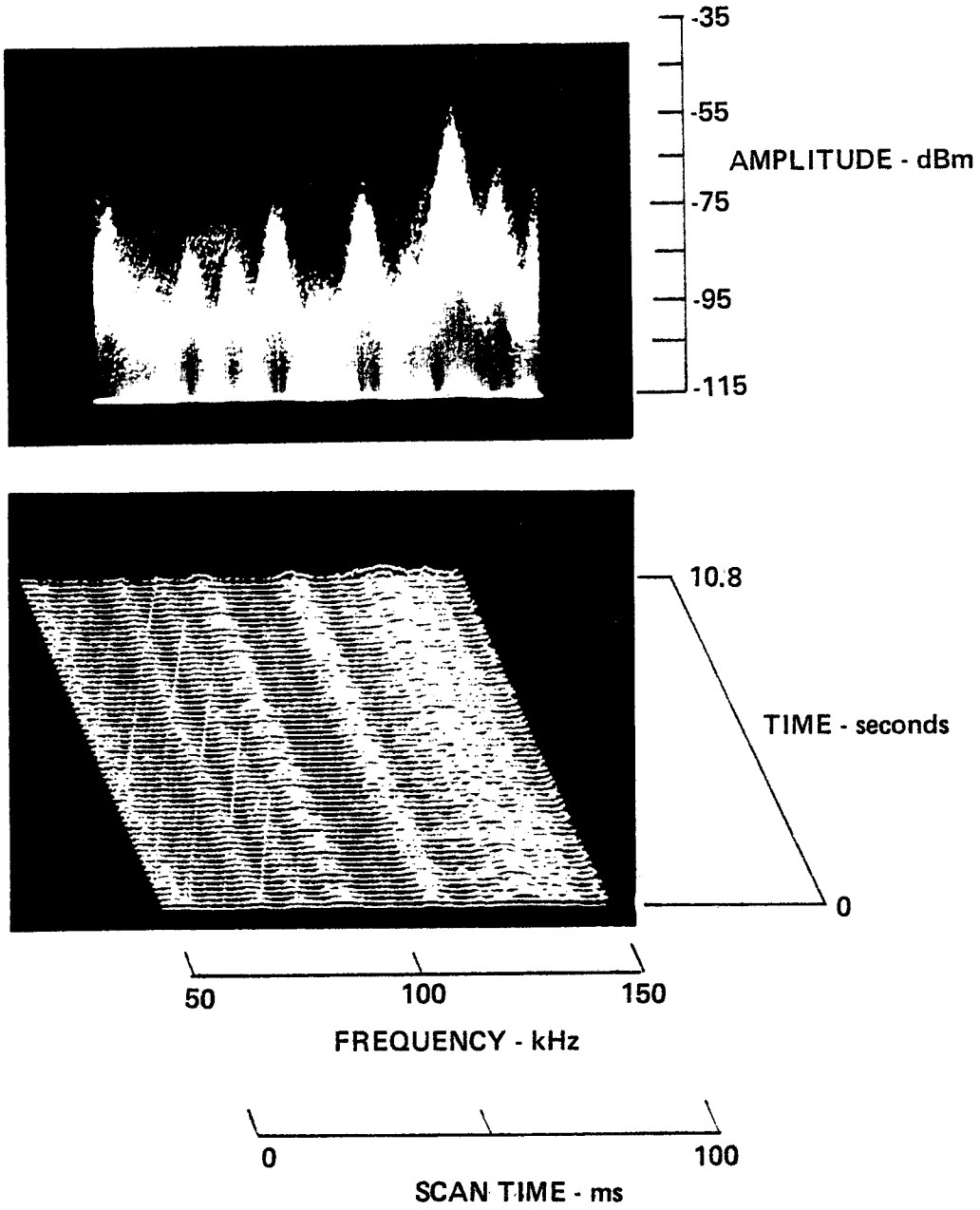

1-25-79, 0914, 110-047
HP140, Whip, F100, W100, IF3, ST 100, A -20/0/+15/NF

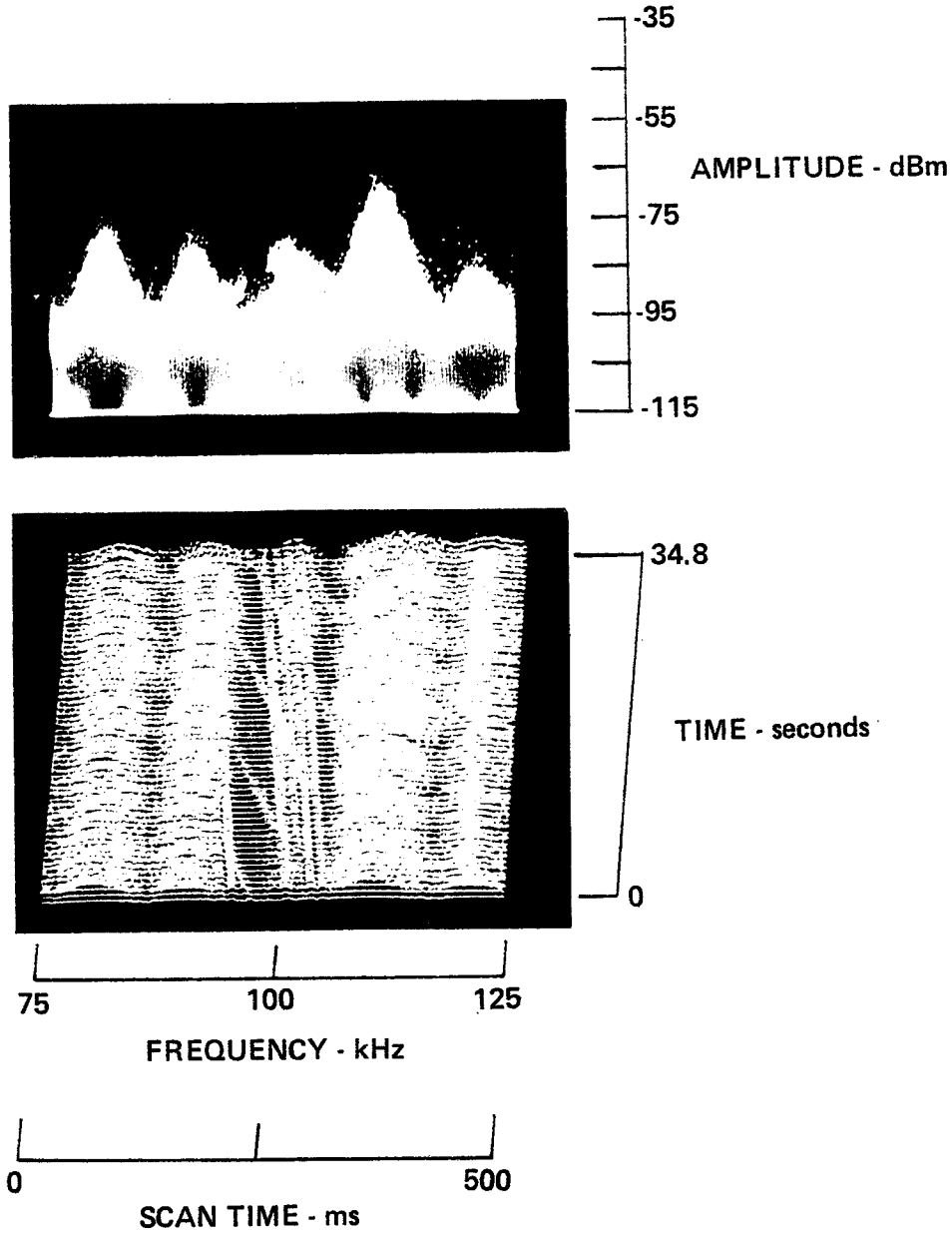

1-25-79, 0932, 110-048
HP140, Whip, F100, W50, IF3, ST 500, A -20/0/+15

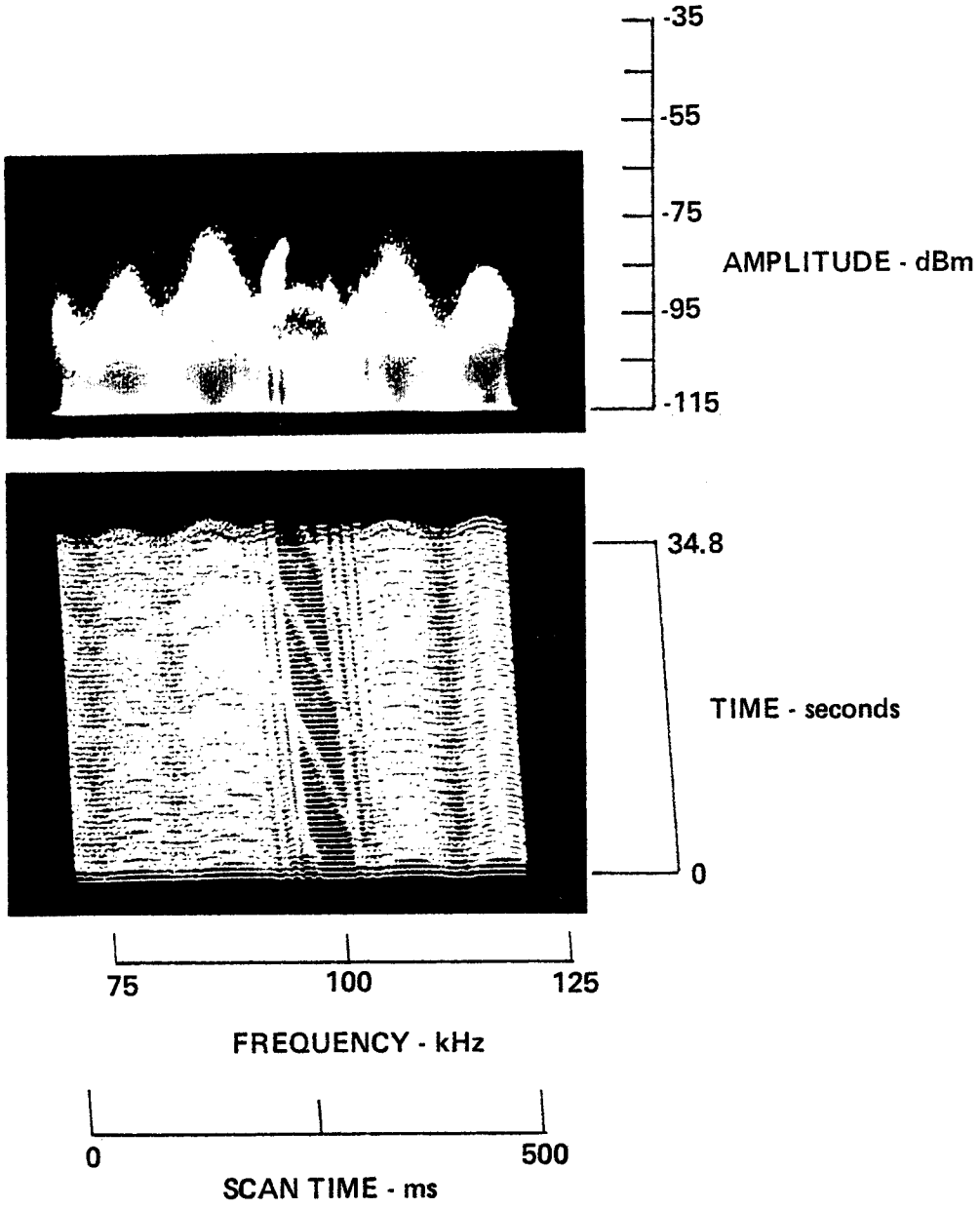

1-25-79, 0948, 110-049
HP140, Whip, F100, W50, IF3, ST 500, A -20/0/+15/NF

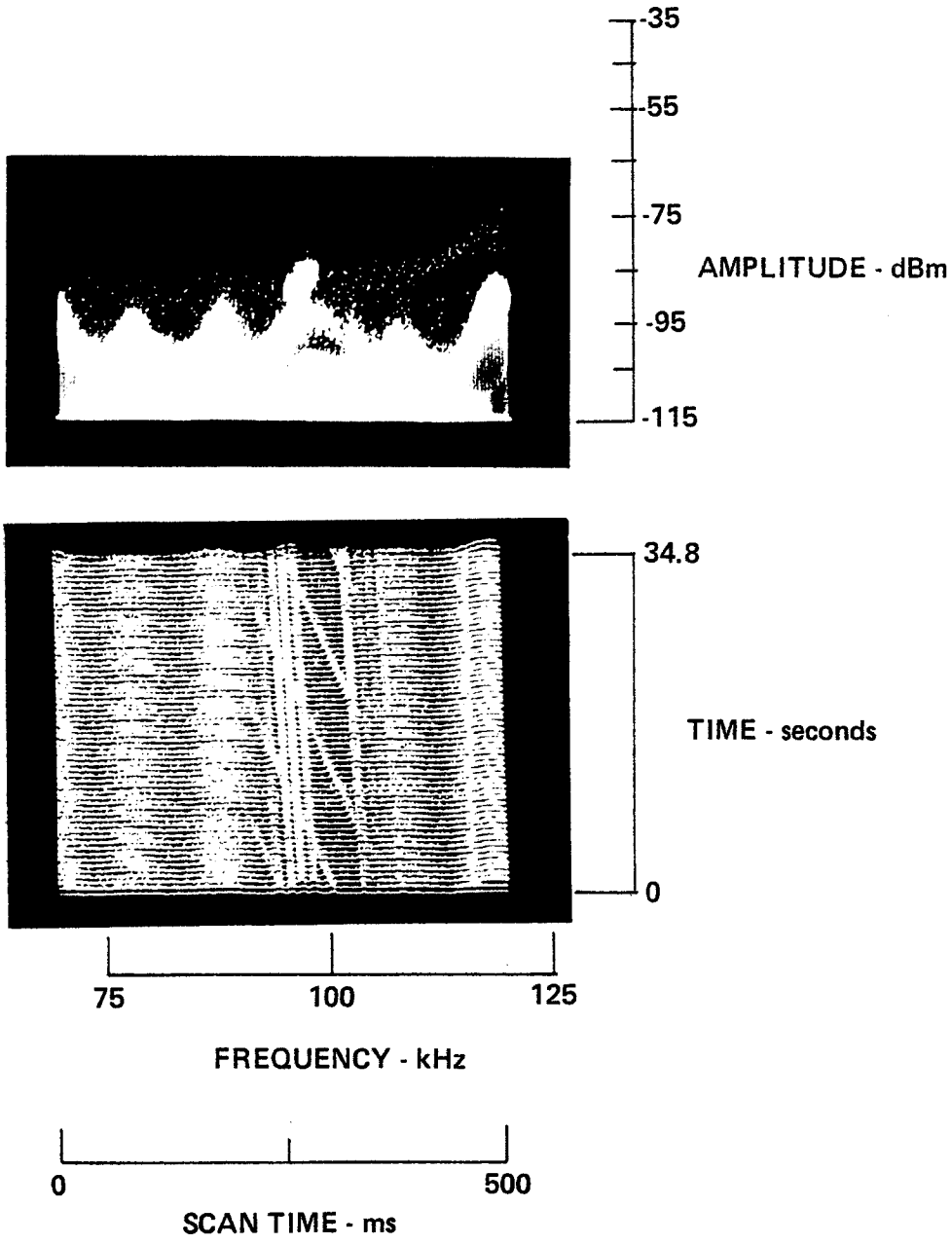

1-25-79, 0958, 110-050
HP140, Whip, F100, W50, IF3, ST 500, A -20/0/+15/NF

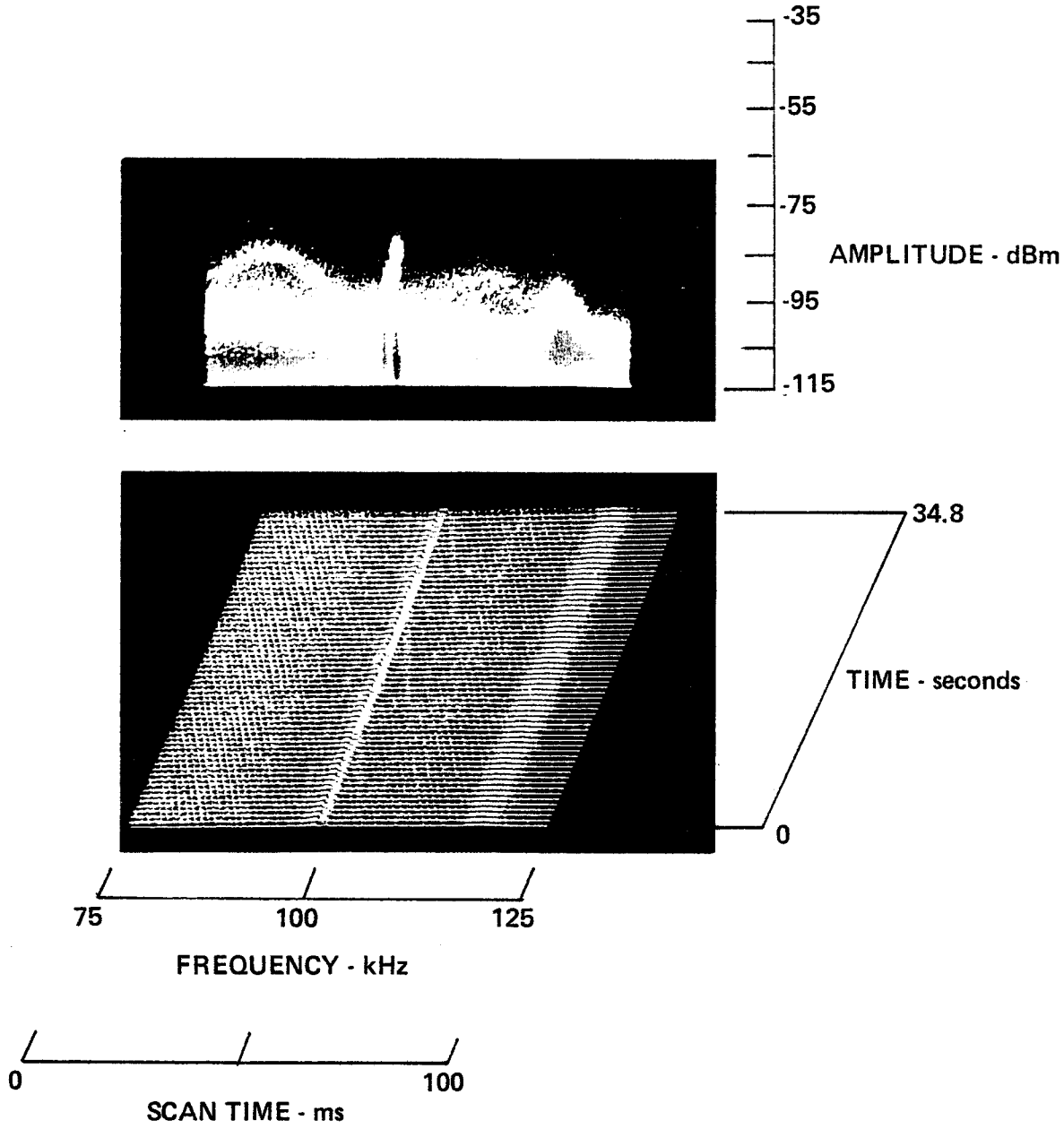

1-25-79, 1228, 104-051
HP140, Whip, F100, W50, IF3, ST 100, A -20/0/+15/NF

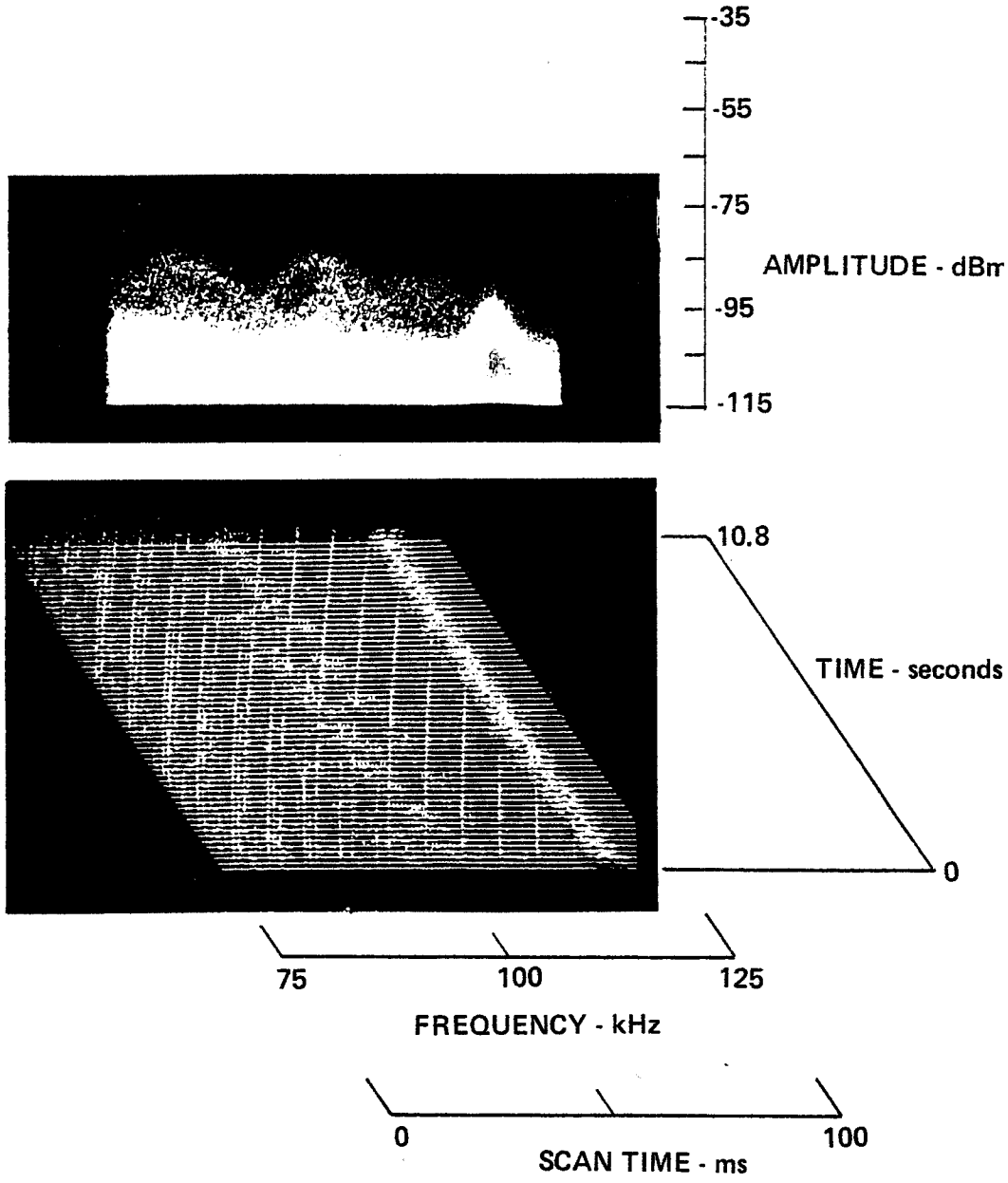

1-25-79, 1227, 104-051
HP140, Whip, F100, W50, IF3, ST 100, A -20/0/+15

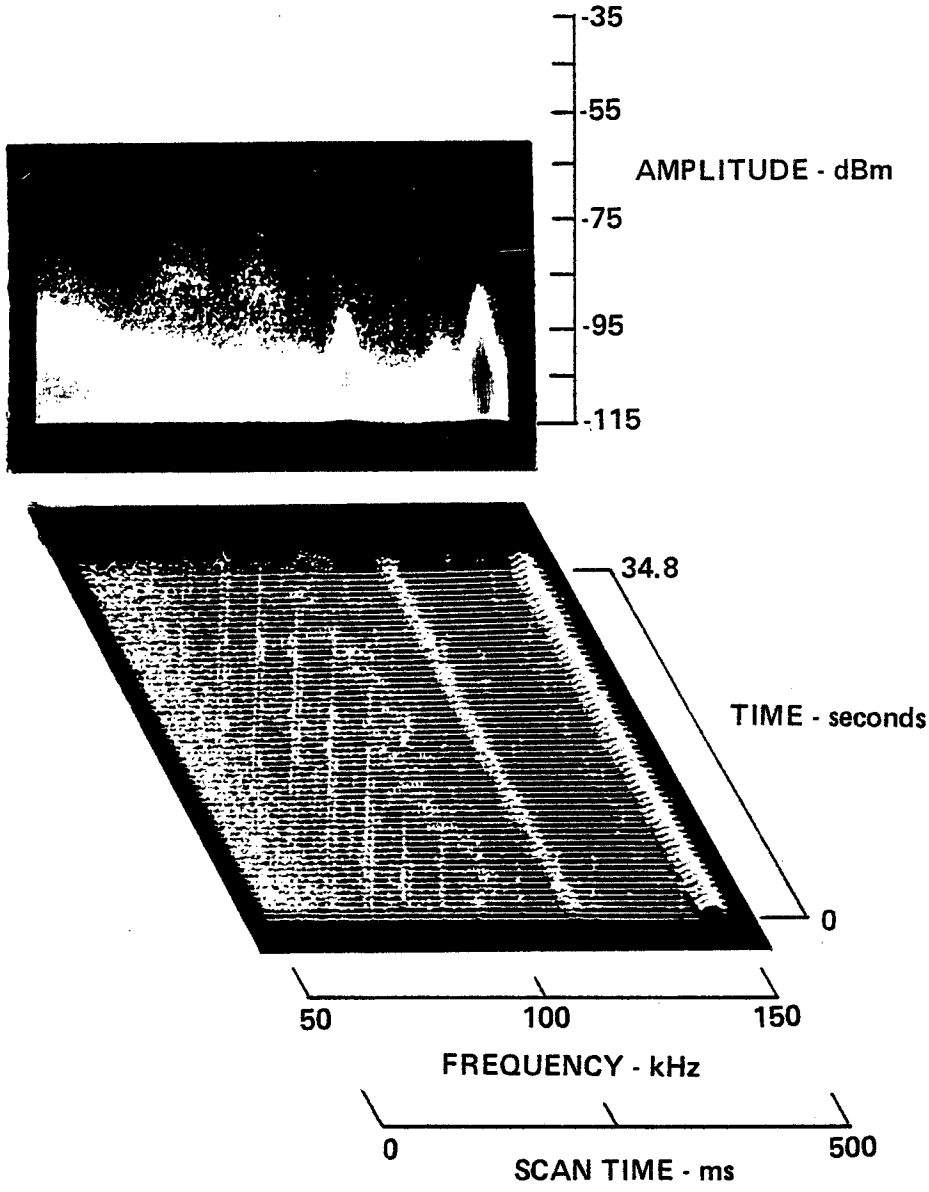

1-25-79, 1230, 104-051
HP140, Whip, F100, W100, IF3, ST 500, A -20/0/+15/NF

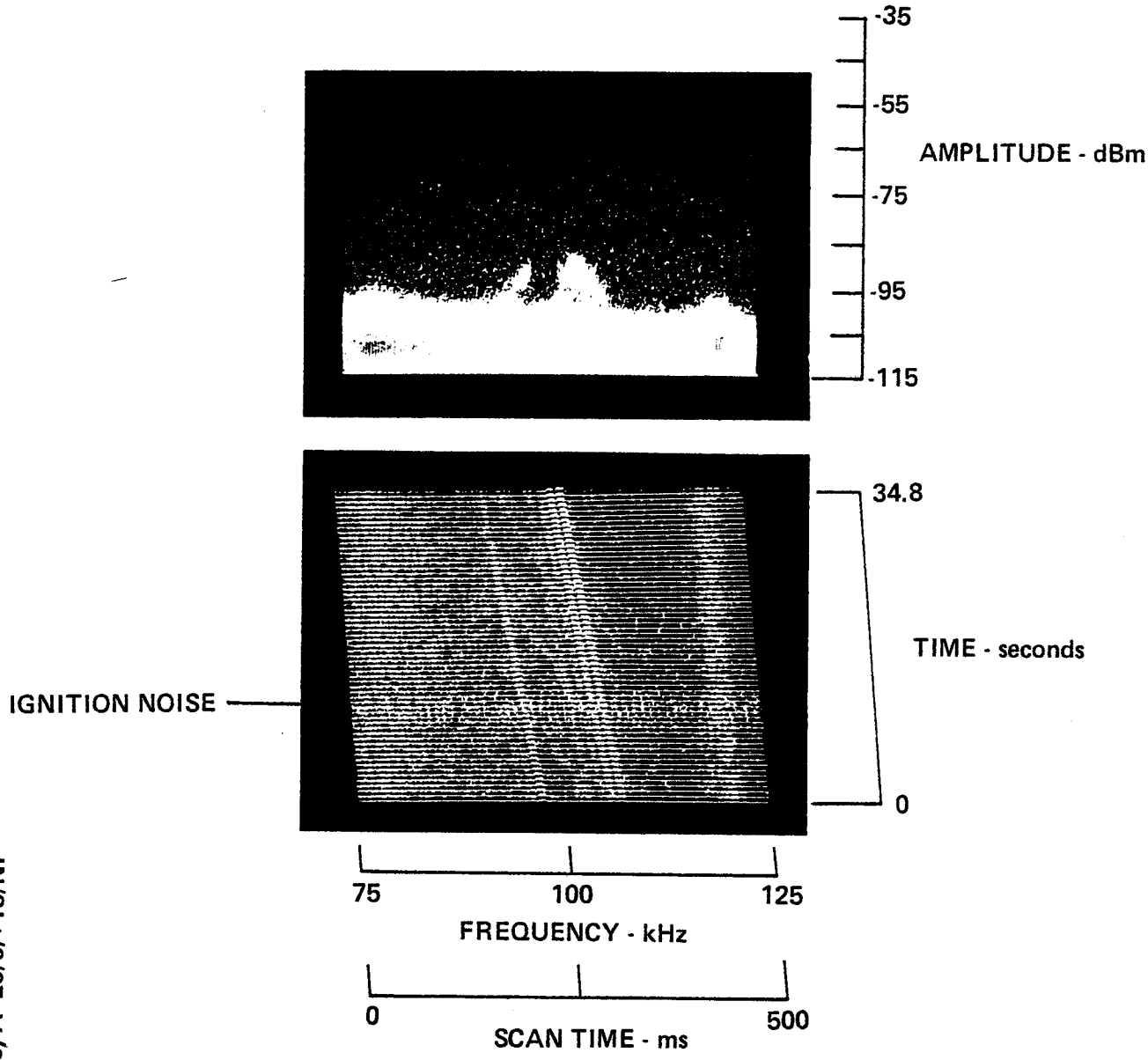

1-25-79, 1238, 104-052
HP140, Whip, F100, W50, IF3, ST 500, A -20/0/+15/NF

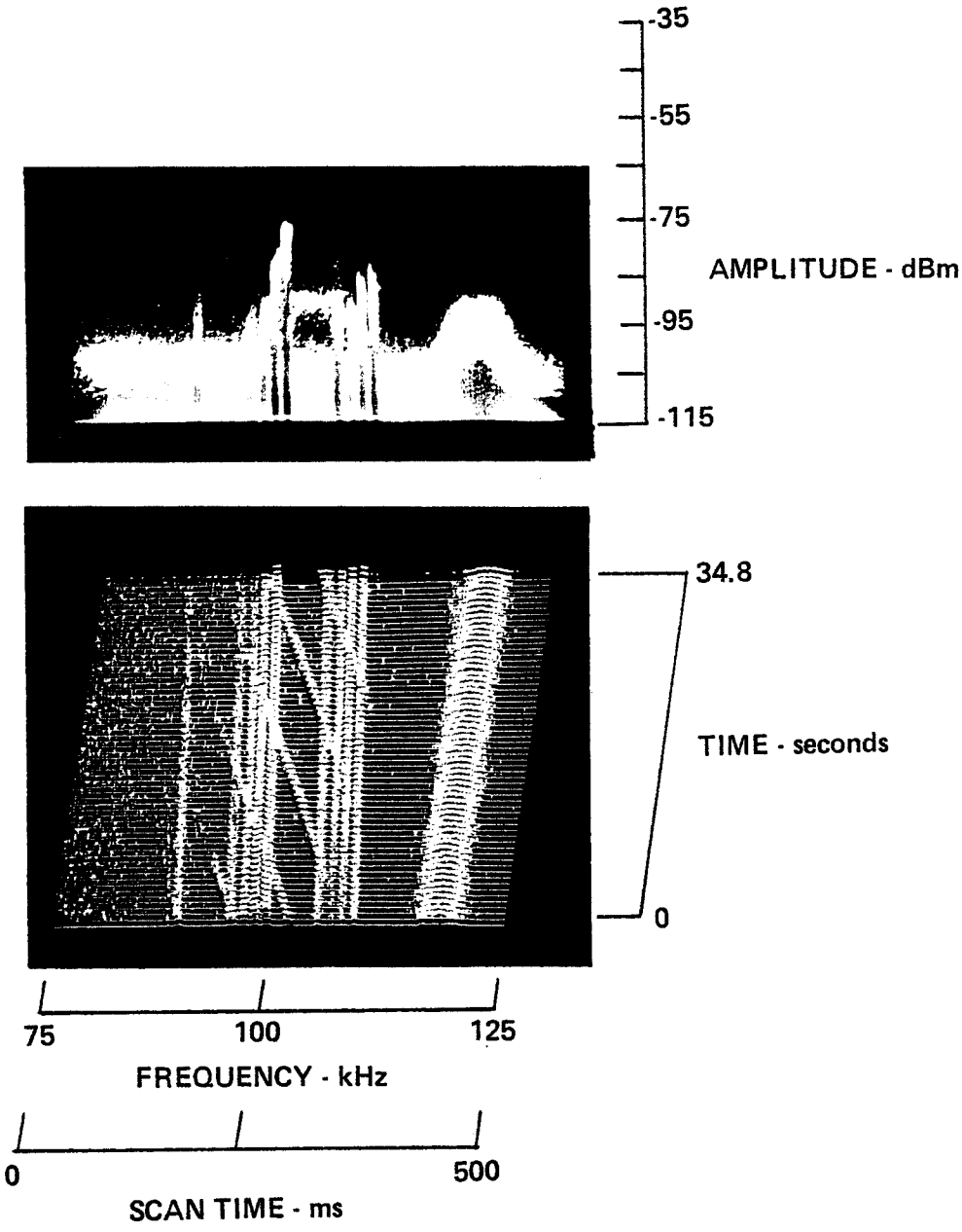

1-25-79, 1253, 104-053
HP140, Whip, F100, W50, IF3, ST 500, A -20/0/+15/NF

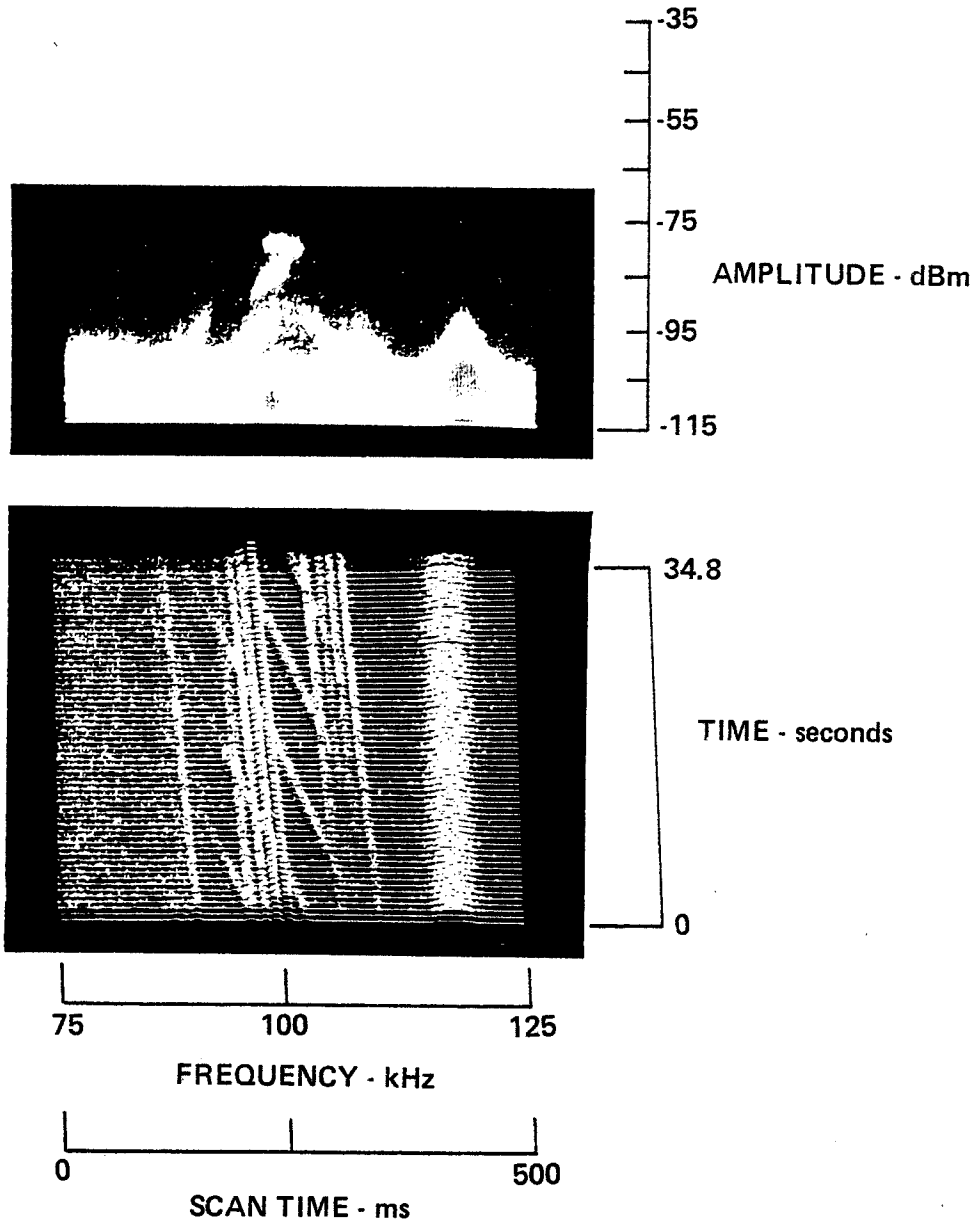

1-25-79, 1306, 104-054
HP140, Whip, F100, W50, IF3, ST 500, A -20/0/+15/NF

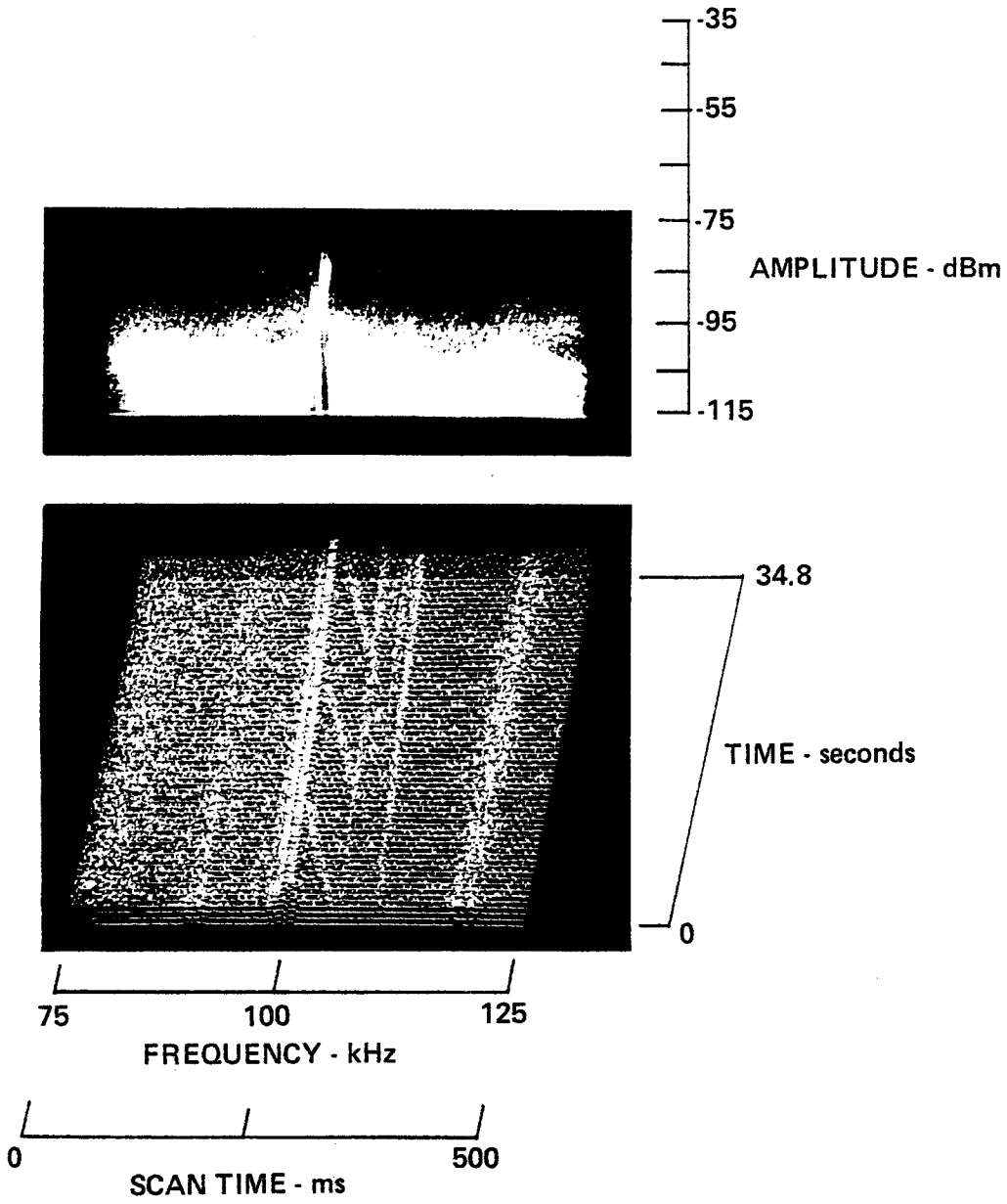

1-25-79, 1322, 104-055
HP140, Whip, F100, W50, IF3, ST 500, A -20/0/+15/NF

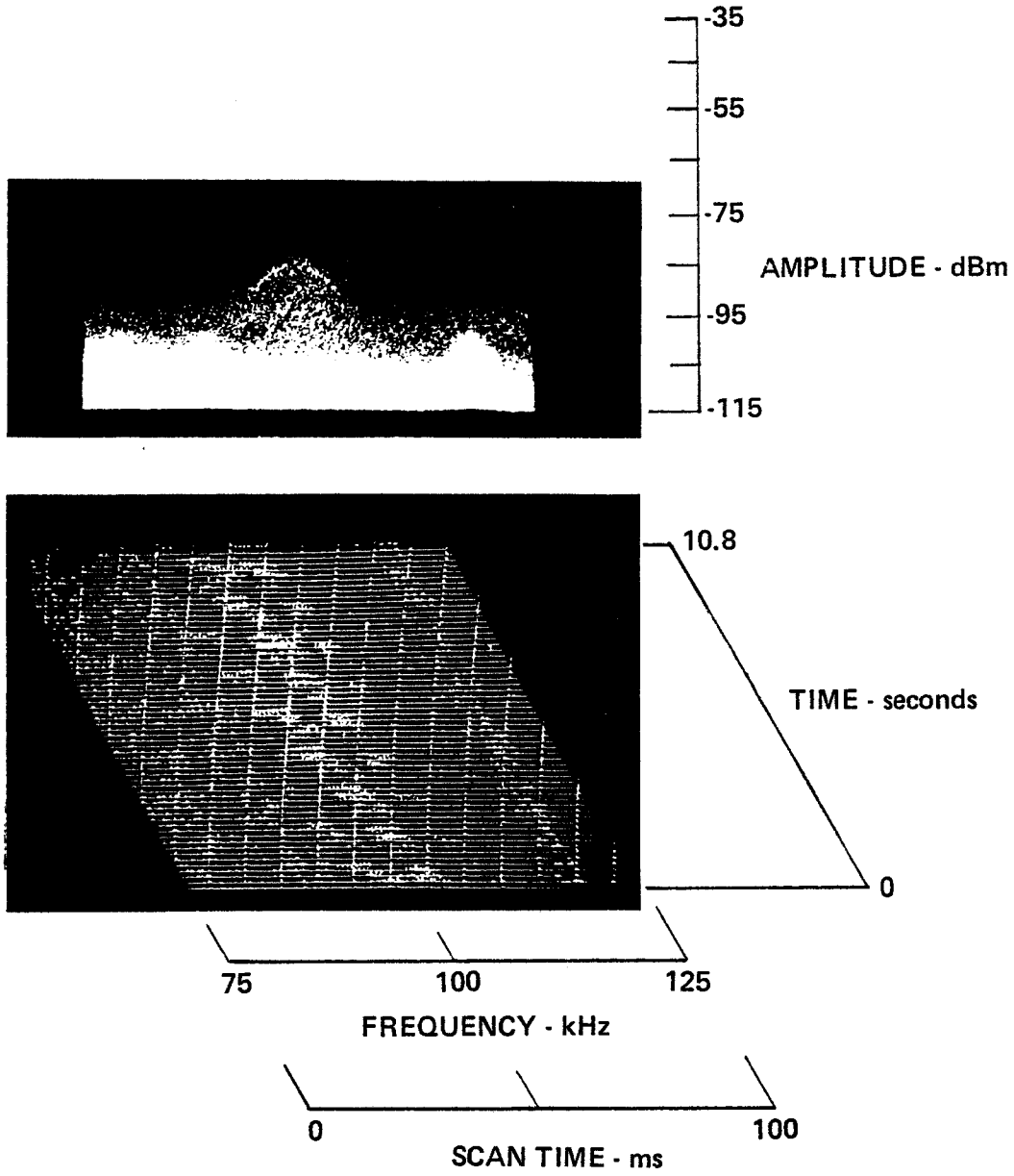

1-25-79, 1321, 104-055
HP140, Whip, F100, W50, IF3, ST 100, A -20/0/+15/NF

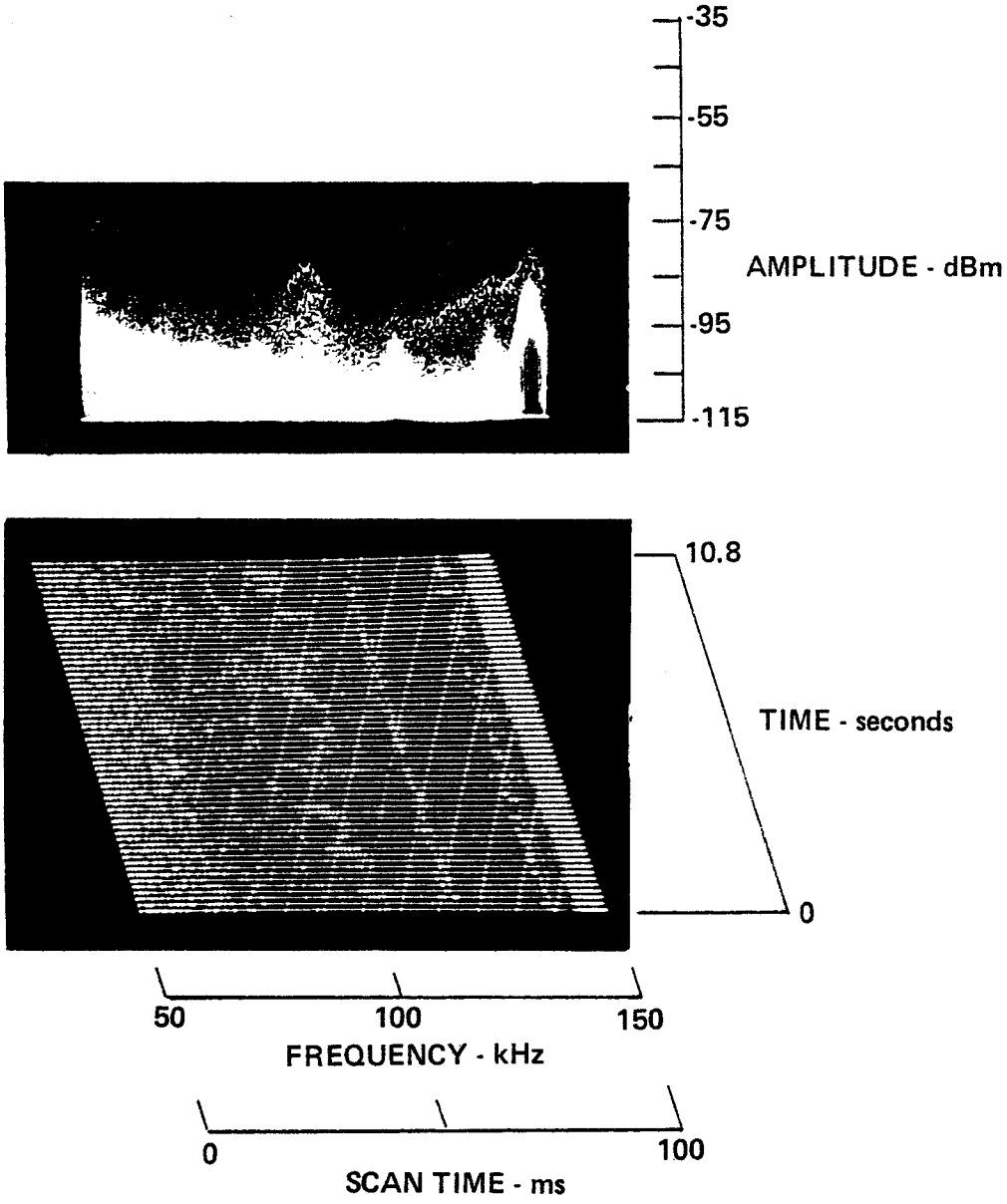

1-25-79, 1325, 104-055
HP140, Whip, F100, W100, IF3, ST100, A-20/0/+15/NF

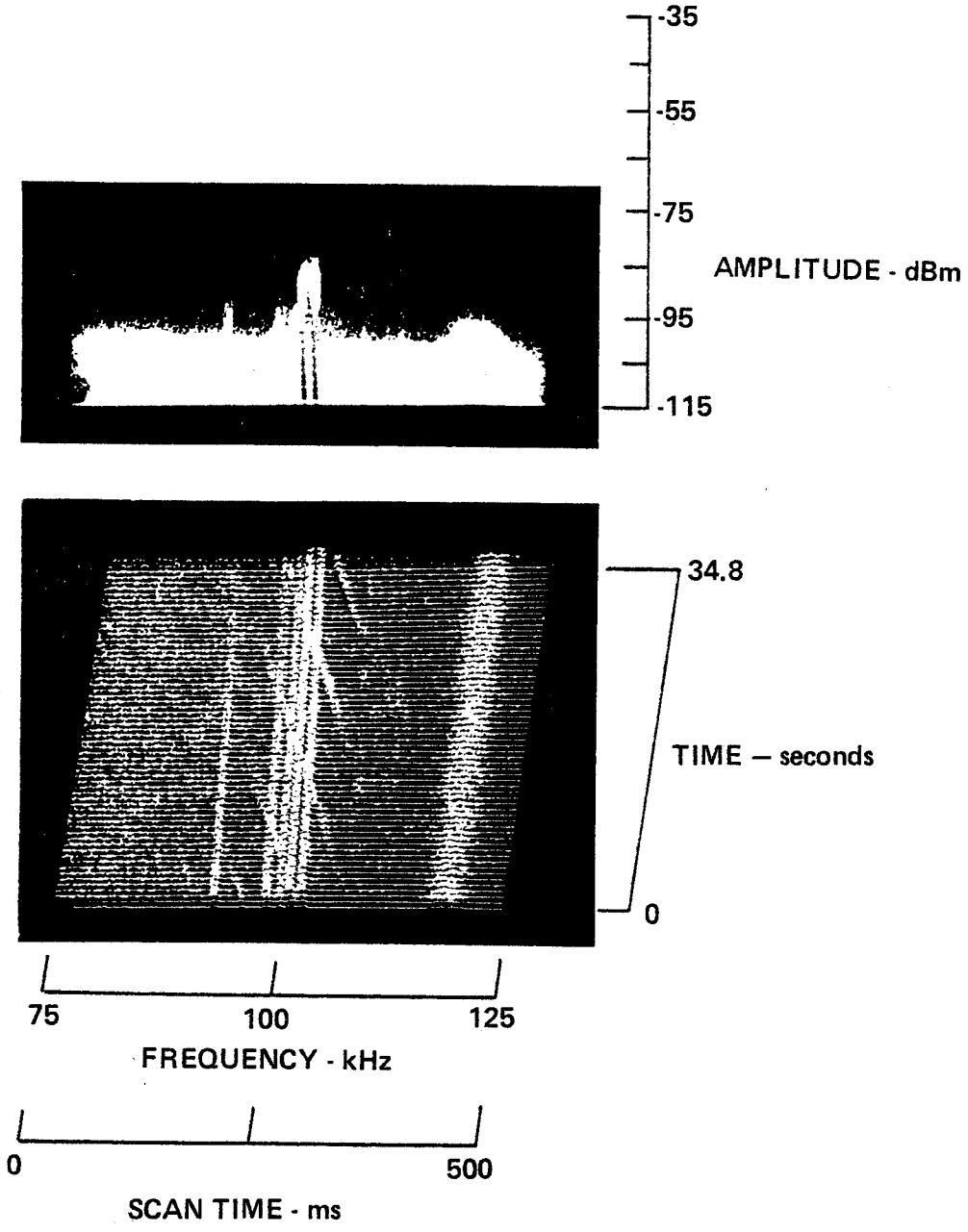

1-25-79, 1332, 104-056
HP140, Whip, F100, W50, IF3, ST 500, A -20/0/+15/NF

APPENDIX B

LIST OF DOCUMENTS USED FOR GENERAL BACKGROUND MATERIAL

1. L.O. Barthold, et al., "Transmission Line Reference Book, 115-138 KV Compact Line Design," Electric Power Research Institute, Palo Alto, California, 1978.

2. R.B. Churchill, "Modeling the Relative Amplitude Probability Distribution of Power Line Noise," ESD-TR-75-019, DoD Electromagnetic Compatibility Analysis Center, Annapolis, Maryland, October 1975.

3. R.A. Shepard and J.C. Gaddie, "Measurement of the APD and the Degradation Caused by Power Line Noise at HF," Final Report, Contract N00039-74-C-0077, Stanford Research Institute, Menlo Park, California, April 1976.

4. Course Text, IEEE Tutorial Course, "The Location, Correction, and Prevention of RI and TVI Sources from Overhead Power Lines," IEEE, New York, New York, 1975.

5. M.S. Gupta, Electrical Noise Fundamentals and Sources, IEEE Press, New York, New York, 1977.

6. R. Caldicott, et al., "Model Study of Electric Field Effects in Sub-Stations," EPRI EL-632, prepared by Ohio State University for the Electric Power Research Institute, Palo Alto, California, January 1978.

7. L.E. Zaffanella and D.W. Deno, "Electrostatic and Electromagnetic Effects of Ultrahigh-Voltage Transmission Lines," EPRI EL-802, prepared by General Electric Company for the Electric Power Research Institute, Palo Alto, California, June 1978.

8. H.N. Shaver, V.E. Hatfield, and G.H. Hagn, "Man-Made Radio Noise Parameter Identification Task," Final Report, Contract N00039-71-A-0223, Stanford Research Institute, Menlo Park, California, May 1972.

9. R.A. Shepard, J.C. Gaddie, V.E. Hatfield, and G.H. Hagn, "Measurements of Automobile Ignition Noise at HF," Final Report, Contract N00039-71-A-0223, Stanford Research Institute, Menlo Park, California, February 1973.

10. Special Issue on Spectrum Management, IEEE Trans. on Electromagnetic Compatibility, Vol. EMC-19, No. 19, August 1977.

11. W.R. Lauber, "Amplitude Probability Distribution Measurements of the Apple Grove 775 KV Project," IEEE Trans. on Power Apparatus and Systems, Vol. PAS-95, No. 4, July/August 1976.

12. A.D. Watt and E.L. Maxwell, "Measured Statistical Characteristics of VLF Atmospheric Radio Noise," Proc. IRE, Vol. 45, pp. 55-62, January 1957.

13. R.A. Shepard, "Measurements of Amplitude Probability Distributions and Power of Automobile Ignition Noise at HF," IEEE Trans. on Vehicular Technology, Vol. VT-23, No. 3, August 1974.

WILBUR R. VINCENT
26070 Kriste Ln.
Los Altos Hills, CA 94022

W R Vincent

SCi
SYSTEMS CONTROL, INC. ■ 1801 PAGE MILL ROAD ■ PALO ALTO, CA 94304 ■ TELEX 348-433 ■ (415) 494-1165

Technical Report No. 4068-250579 May 1979

IMPULSIVE NOISE IN THE 3 TO 300 kHz BAND ON ELECTRIC UTILITY DISTRIBUTION LINES FROM A 1.6 MW EXPERIMENTAL CONVERTER BRIDGE

Prepared for:

McGraw-Edison Co.
P.O. Box 440
Canonsburg, Pennsylvania 15317

Under:

Electric Power Research Institute
Contract RP 1024-1

Prepared by:
W.R. Vincent

TABLE OF CONTENTS

TABLE OF CONTENTS (Continued)

LIST OF FIGURES

LIST OF FIGURES (Continued)

LIST OF TABLES

Section 1

INTRODUCTION

Under EPRI Contract RP1024-1, the Power Systems Division of the McGraw-Edison Company, Canonsburg, Pennsylvania, was tasked with the measurement of harmonic voltage and current levels on Connecticut Light and Power (CL&P) distribution lines which were tied to a 1.6 MW experimental converter bridge located at the United Technology Corporation (UTC) Power Systems Division facility in South Windsor, Connecticut. McGraw-Edison subcontracted with Systems Control, Inc. (SCI) of Palo Alto, California, to measure electrical noise levels on the CL&P distribution lines at frequencies above conventional harmonic measurements. The SCI measurements were made primarily at frequencies commonly called very low frequencies (VLF) covering the 3 to 30 kHz range and the low frequencies (LF) covering the 30 to 300 kHz band. A few exploratory measurements were made above and below the VLF and LF bands in order to provide a comprehensive understanding of observed noise properties.

The SCI VLF and LF measurements were conducted simultaneously with the harmonic measurements of McGraw-Edison. These measurements complemented and supplemented the McGraw-Edison harmonic measurements by extending the frequency range upward and by the use of additional instrumentation to define noise properties.*

The measurements described in this report were, to a large extent, exploratory in nature. A literature search did not reveal significant data which directly applied to the CL&P/UTC type of situation. Thus, it was necessary to adopt an iterative measurements procedure where measurement system parameters were adjusted as experience was gained throughout the measurements period. Both McGraw-Edison and SCI field measurement

---

* The term impulsive noise has been used in this report because it can be physically related to primary properties of the observed noise. The relationship between the term "impulsive noise" and "higher order power line harmonics" or "higher order harmonics of the power line frequency" is discussed in Section 4.5.

personnel realized that a significant opportunity existed to relate a specific and controlled source of harmonic and noise energy to harmonic and noise levels on the associated distribution lines. An excellent working arrangement rapidly developed between the various parties involved in the effort, including CL&P, UTC, McGraw-Edison and SCI personnel, which permitted the investigation to be accomplished efficiently and with reasonable depth.

Section 2

INSTRUMENTATION

Instrumentation used to acquire data presented in this report was adapted from equipment used for previous field measurements where little was known about the frequency or time domain properties of signals or noise [1-3]. A frequency scanning receiver was employed to observe noise amplitude across large blocks of frequencies where the scanning process was also employed to aid in defining the time domain structure of the wideband noise under observation. Figure 1 shows a block diagram of the primary instrumentation components.

Simple whip or loop antennas were employed for most measurements to sense the electric or the magnetic component of the field around the transmission line caused by impulse voltage and current on the line. The antennas were placed directly under the transmission line in the inductive or near field region. In addition, the instrumentation was occasionally connected directly to voltage probes and current sensors attached to the distribution line by McGraw-Edison for harmonic measurements.

A Hewlett-Packard 140 Spectrum Analyzer was employed as a scanning receiver to drive an EMTEL Model 7200B 3-Axis Display. The 3-axis display provided a moving real-time visual representation of noise received by the scanning receiver.

To acquire data the spectrum analyzer was adjusted to scan across a desired block of frequencies. As the spectrum analyzer scanned through a block of frequencies, its output was divided by the 3-axis display into 512 equally spaced data points. The received signal or noise amplitude at each data point was represented by an 8-bit digital word which provided an amplitude resolution of 256 levels for each data point. When a scan was completed, the 512 amplitude words were stored in memory and then presented as line 1 on the display CRT. When the

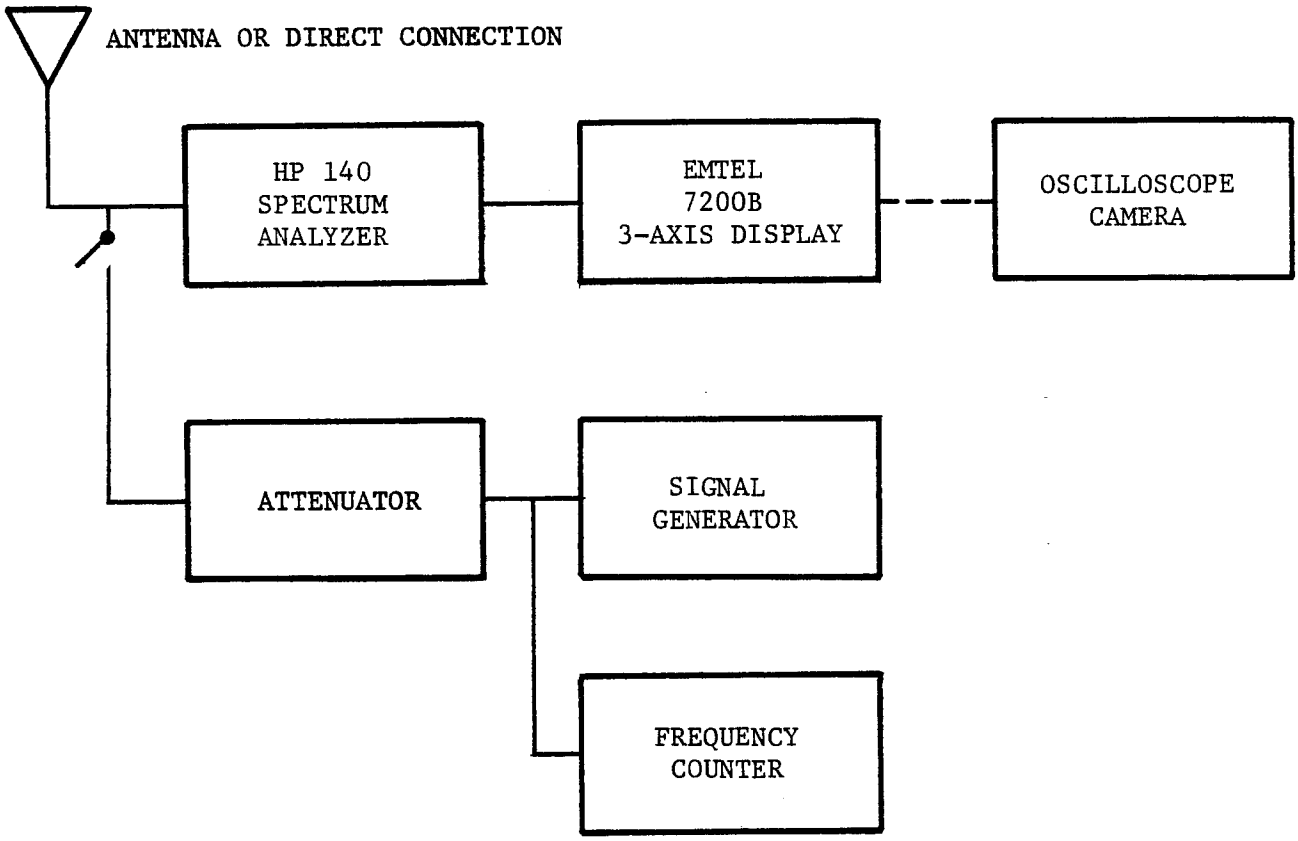

Figure 1 Block Diagram of Primary Instrumentation Components

second scan was completed, its data were stored in memory, line 1 on the CRT moved to line 2, and the new scan was shown on line 1. Subsequent scans moved the earlier data lines step by step along the time axis until the entire memory was filled and a total of 60 scan lines were presented in the 3-axis view. When the memory was full, each new scan caused the oldest scan to be discarded. The resulting animated moving view of signals and noise provided a unique and easy-to-interpret visual picture of noise and signals in the blocks of frequencies under observation.

The 3-axis display system has a number of controls to assist the operator in interpreting the signals. Among these controls are a stop-action control to freeze any desired view for detailed observation, geometry controls to vary the viewing aspect, display mode controls to select any segment of the total view for detailed examination, and a threshold control to vary the background noise level.

The 3-axis views presented in this report were obtained by photographing the display in its stop-action mode. In interpreting the data, consideration must be given to situations where repetitive impulsive signals are observed by the repetitive scanning process. The relative repetition rates of impulsive signals and the scan rate of the receiver produce distinctive bands that slant across the CRT.

The instrumentation was installed in a small self-contained van for mobility and convenience in travel from site to site. Usually, electrical power was provided by CL&P personnel. When power was not available a small gasoline-powered generator was used to operate the instrumentation.

Section 3

MEASUREMENTS

3.1 GENERAL APPROACH

Prior to the data collection period of 6/26/78 to 6/29/78, McGraw-Edison and CL&P personnel conducted a survey of all sections of the 13.8 kV distribution system which might be impacted by harmonic levels from the UTC experimental bridge converter. Tentative measurement sites were selected during these early surveys which proved to be excellent sites for the measurement and data collection program described in this report.

Instrumentation for the McGraw-Edison harmonic measurements was installed in a small van similar to the SCI van used for higher frequency data collection. Both vans, accompanied by CL&P line crews and supervisory staff, moved to the appropriate site, operated the instrumentation for data collection and then moved to the next site. CL&P personnel provided suitable 115 volt, 60 Hz single phase power for instrument operation, communications to the UTC plant, coordination with CL&P facilities, and other support tasks.

Polaroid photographs of pertinent 3-axis display presentations were made to record the noise and signal structure for each test condition. Many of the Polaroid photographs taken in the measurements were selected for presentation in this report. Usually a pair of photographs at two separate viewing aspects was made to better portray all important properties of the observed noise. The versatility of the display in presenting the observed data in viewing aspects which maximized the visual perception of important structures was found to be very useful.

All 3-axis views were accurately calibrated in frequency, amplitude, and time. The frequency and time scales are obvious, except

that the horizontal frequency axis in all views is also associated with scan time. A bandpass filter, the scanning receiver IF bandwidth, was moved across the frequency axis from minimum frequency to maximum frequency at a scan time greater than several complete cyles of the 60 Hz power line frequency. Thus, several repetitive and sequential impulses associated with the power line frequency appeared on each scan. This combined frequency and scan time property of the instrumentation was found to be highly useful in the data analysis. All instrumentation operating parameters employed to obtain each view have been provided in convenient tabular form to aid in the scaling of the 3-axis views by interested readers.

Signal amplitude has been expressed in terms of dB below 1 milliwatt at the spectrum analyzer 50 ohm impedance input in all 3-axis views. For those views employing the 108" whip antenna, the dBm scale can be converted into an equivalent field strength in volts/meter by the following conversion:

$$p_n = f_a(k\ T_o\ b)$$

where p_n = mean noise power in watts

f_a = effective antenna noise factor

k = Boltzman's constant τ $1.38 \cdot 10^{-23}$ Joules/°K

T_o = reference temperature (288°K)

b = receiver noise power bandwidth in Hz

T_a = effective antenna temperature in the presence of external noise.

The above expression for p_n can be reduced to:

$$P_n = F_a + B - 204 \quad \text{dBw}$$

which is the power available from the terminals of an equivalent lossless antenna where

P_n = available noise power in dBw

$F_a = 10 \log f_a$, the effective antenna noise figure

$B = 10 \log b$.

The corresponding rms field strength measured by the 108" whip antenna (length $<< \lambda$) is given by:

$$E_n = F_a + 20 \log f + B - 95.5 \quad \text{dB}(1\mu\text{V/m})$$

where E_n = rms field strength for the bandwidth b

f = frequency in MHz

$B = 10 \log b$.

The amplitude scales for the 3-axis views in this report can be recalibrated in terms of either P_n or E_n from the above relationships and from data contained in the tables of system parameters provided with the views.

3.2 PHYSICAL DESCRIPTION

A diagram showing the primary features of the CL&P distribution lines between the substation power source and the UTC converter is shown in Figure 2. This diagram shows all interconnected distribution lines, power factor correction capacitors, measurement sites, and the distance between each major section. Figure 2 was extracted from the McGraw-Edison master report which describes the related measurements of harmonic voltage and current levels. The McGraw-Edison master report contains more detailed information on the distribution system, photographs of each site and other pertinent data. Sufficient data were extracted from the master report to provide a consistent and self-contained document describing noise results. All site names and other site information are consistent with those in the master report to simplify the task of correlating the results of the two measurement efforts.

VLF/LF radio noise on the distribution line was examined at each measurement site starting with the UTC Riser Pole site immediately opposite from the UTC Power Systems Division Facility and followed in sequence at the Substation Entrance site, Spring Pond site, Vulcan Radiator site and the Feeder 4 site. Noise levels were examined at each site with the converter both on and off. In addition, noise levels were measured as the 1200 kVAR capacitor bank near the UTC Pole and the 600 kVAR capacitor bank near the Spring Pond site were switched in and out. The various combinations of converter on/off and capacitor bank in/out which were investigated are given in Tables 1 through 5.

Instrumentation check-out measurements were made on 6/26/78, the day before the start of joint McGraw-Edison/SCI site measurements, at the rear of the UTC facility near Gatehouse 3. These measurements permitted the instrumentation to be checked and field-calibrated prior to actual site operation. A full day was allowed for instrumentation check-out to detect and correct any possible difficulties from shipment

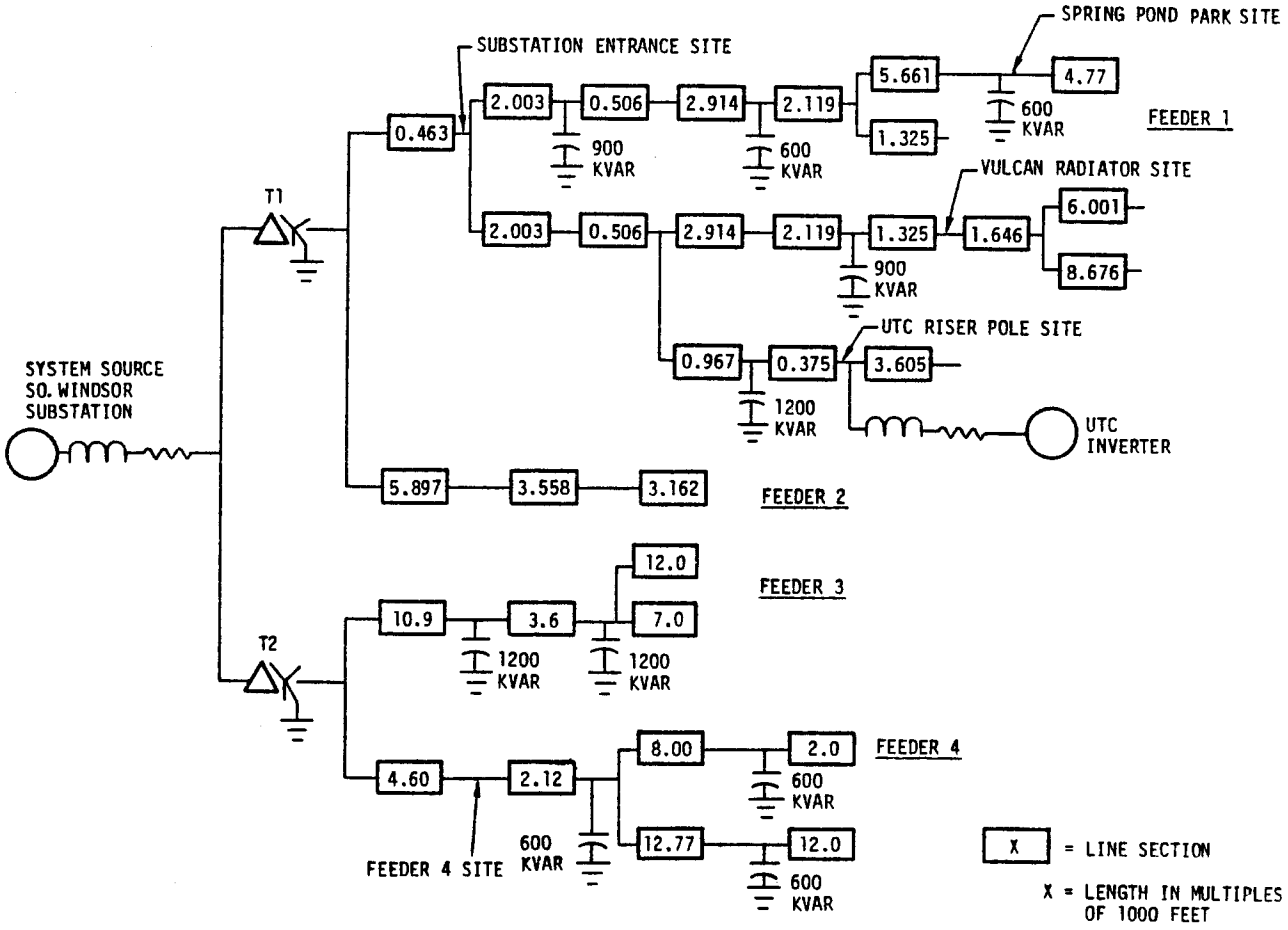

Figure 2 CL&P System Diagram

across country. Since equipment difficulty was not encountered, the instrumentation was used to explore background radio noise near the UTC facility. These early measurements proved to be of considerable value in understanding general background noise properties. Most noise was impulsive, with impulses synchronous with the power line frequency. The complexity of the background, and the unusually large frequency range with significant levels of impulsive noise was unexpected. The Gatehouse 3 measurements were of considerable value in establishing preliminary instrumentation operational parameters, and the results were consistent with subsequent site measurements. Therefore, Gatehouse 3 noise examples have been included in this report immediately after the site measurements.

3.3 UTC RISER POLE SITE

3.3.1 Measurement Conditions

The UTC Riser Pole site was selected for the first set of measurements because of its close proximity to the UTC plant and the UTC experimental converter bridge. The site was located across the road from the main UTC Power Systems Division buidling. An underground cable ran from the riser pole to the UTC plant distribution gear which connected the 1 MW converter to the CL&P system as well as all other plant loads. A 1200 kVAR capacitor bank also identified with the UTC Riser Pole site was 375' from the riser pole in the direction of the CL&P system source.

The SCI measurement van was placed directly under the 13.8 kV distribution line near the riser pole. Loopstick and whip antennas were employed to sense electric and magnetic fields from electrical noise on the line. Measurements were made at the UTC Riser Pole site on 6/27/78 from 0800 to 1600 hours local time.

Measurement system parameters for the various 3-axis views taken at the UTC Riser Pole site are summarized in Table 1. These parameters will be useful to those individuals who wish to scale the 3-axis views for some specific detail.

Table 1

MEASUREMENT PARAMETERS, UTC RISER POLE SITE

FIG. NO.	DATE	LOCAL TIME	ANTENNA	FREQ. CENTER kHz	FREQ. WIDTH kHz	IF BAND-WIDTH kHz	SCAN TIME ms	IF REF. dB	RF REF. dB	CAP. UTC	CAP. S.P.P.	UTC CONV.
3	6/27/78	1132	Loop	200	100	1	100	-30	0	on	on	on
4	6/27/78	1033	Loop	450	200	3	100	-40	0	on	on	off
5	6/27/78	1149	Loop	1000	50	3	100	-30	10	on	on	on
6	6/27/78	1157	Whip	1000	50	3	100	-40	0	on	on	on
7	6/27/78	1126	Loop	50	50	1	100	-30	0	on	on	on
8	6/27/78	1423	Loop	70	50	1	100	-20	0	on	off	on/off
9	6/27/78	1400	Loop	30	20	1	100	-20	0	off/on	on	on
10	6/27/78	1443	Loop	50	50	1	100	-20	0	on/off	on	on
11	6/27/78	1449	Loop	50	50	1	100	-20	0	off/on	on	on
12	6/27/78	1520	Loop	60	100	1	100	-30	0	on	on	off/on

3.3.2 Background Measurements

Background noise levels were examined prior to the converter tests to explore possible noise and signal structures on the overhead distribution line from sources other than the converter. The background measurements showed that significant levels of impulsive noise existed on the line before the converter was turned on. This noise was used to check instrument operation and antenna orientation and to establish general instrumentation operational procedures.

Figures 3 through 5 show typical background impulsive noise signatures at various frequency bands. An examination of Table 1 shows that the inverter was on during the time Figures 3, 5 and 6 were taken; however, the noise shown was from other background sources. Noise energy peaks were found centered at about 225, 470, 540 and 1000 kHz. The straight lines in the skewed views parallel to the time axis are signals from power carrier communications systems operating on nearby utility transmission lines and distant radio stations also received by the exposed loopstick sensors. The radio signals aided in checking frequency and amplitude calibration of the system, but they can be ignored for impulsive noise interpretation purposes.

The bottom view of Figure 5 shows a somewhat blurred and indistinct slanting line upward and across the view. These slanting lines were formed by the interaction of the frequency scanning receiver with the repetitive impulsive properties of the noise source. The noise peaks were spaced about 2.8 ms apart, implying that the source was an impulse device triggering on the positive and negative portions of the voltage cycle of a three-phase system. The blurred nature of the noise peaks suggested that the trigger point of the impulse device varied somewhat with respect to phase of the electrical power.

The upper view of Figure 5 shows the same data contained in the lower view but with the display controls changed. The vertical aspect

was set to 0°, the horizontal aspect to 0°, and the amplitude compression was removed. The upper view shows amplitude of the impulse noise vs. frequency. Amplitude peaks were spaced about 9 kHz apart. These peaks imply that the source-to-radiation mechanism of the line contained a 9 kHz electrical resonance creating standing waves on the overhead transmission line. The two views of Figure 3 provide a comprehensive means to examine primary features of the impulsive noise in both the time and frequency domains.

Figure 4 shows the properties of impulsive noise at about 470 kHz. The bottom view shows very distinct lines slanting upward through the view compared to those of Figure 3. These distinct lines were also spaced about 2.8 ms apart near 470 kHz, but they were spaced 8.3 ms apart at about 547 kHz. Two distinct noise amplitude peaks can be identified in the upper view at 470 and 540 kHz which were associated with the two spacings identified in the lower view. The views of Figure 4 suggest that two sources contributed to the impulsive noise where both sources had very stable trigger points with respect to phase of the power system. The source of the 470 kHz noise was associated with a three-phase device and the source of the 540 kHz noise was a single phase device.

The 3-axis views of Figure 5 show another noise signature near 1000 kHz. The lower view shows slanting lines spaced 16.6 ms apart along with other diffuse but synchronized noise peaks at closer intervals. Either multiple sources were involved or a complex single noise source existed to produce the complex view. The 16.6 ms spacing implied a single phase source with triggering on either the positive or negative portion of the 60 Hz power line frequency. The diffuse closer spaced detail implied that a three-phase source also existed.

Figure 6 is identical to Figure 5 except that the whip antenna was employed in place of the loop antenna used for the views in Figures 3 through 6. The detail shown in Figure 6 is similar to that of the comparable measurement in Figure 5 except for a lower amplitude.

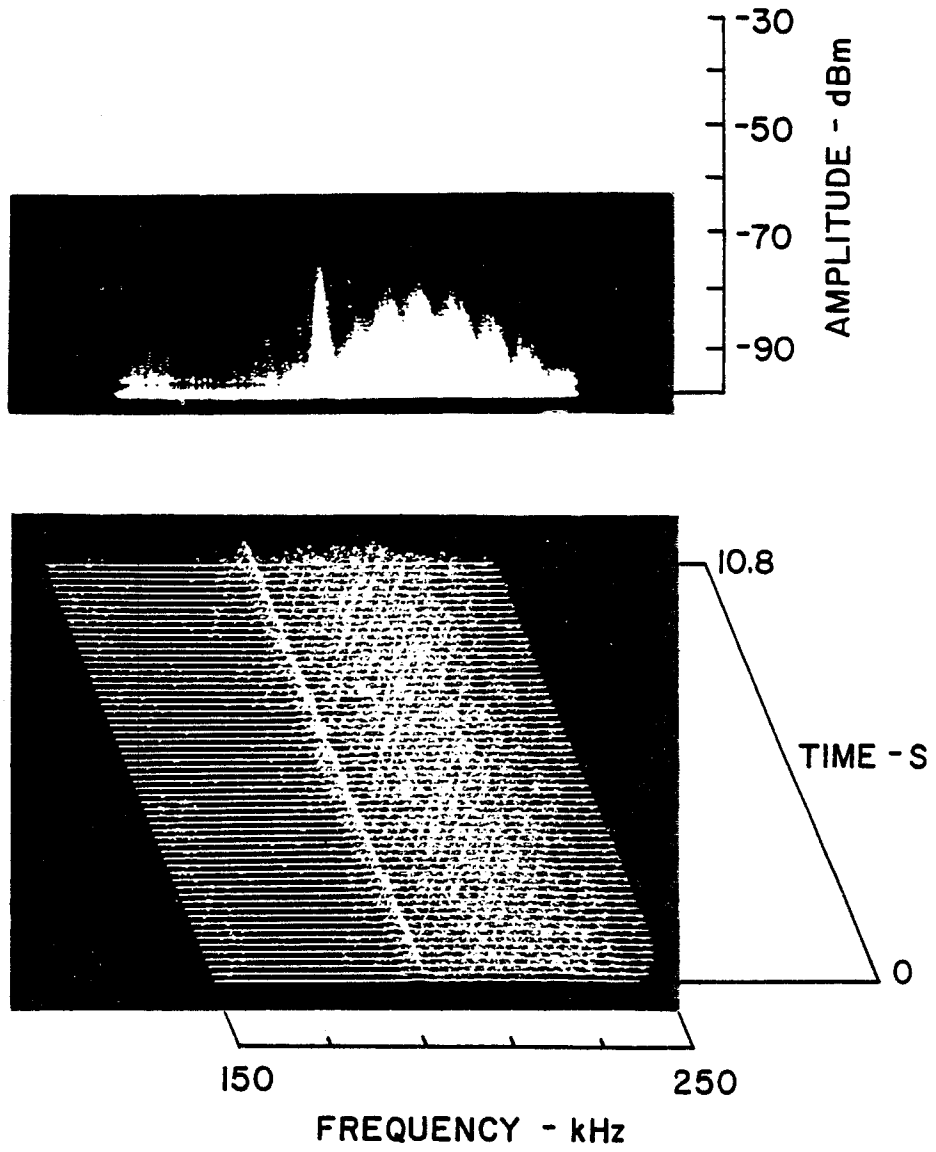

Figure 3 UTC Riser Pole Site, 6/27/78, 1132

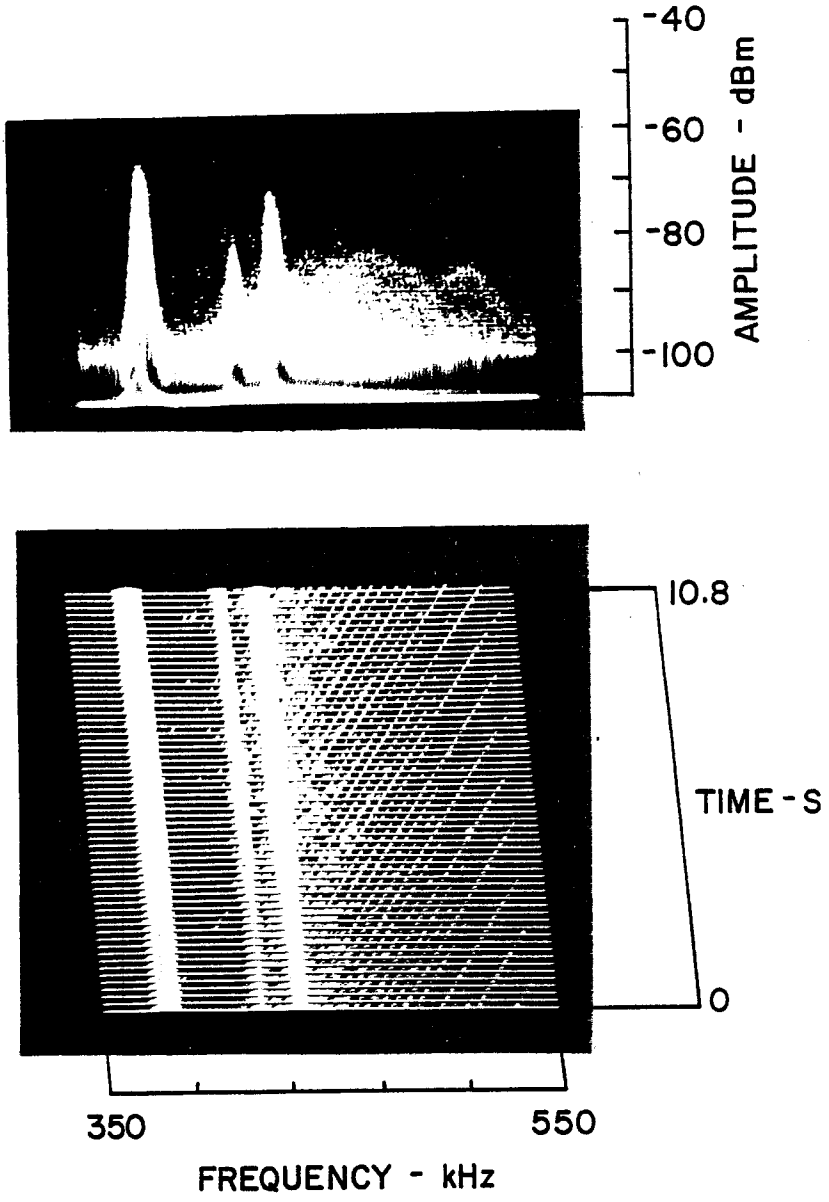

Figure 4 UTC Riser Pole Site, 6/27/78, 1033

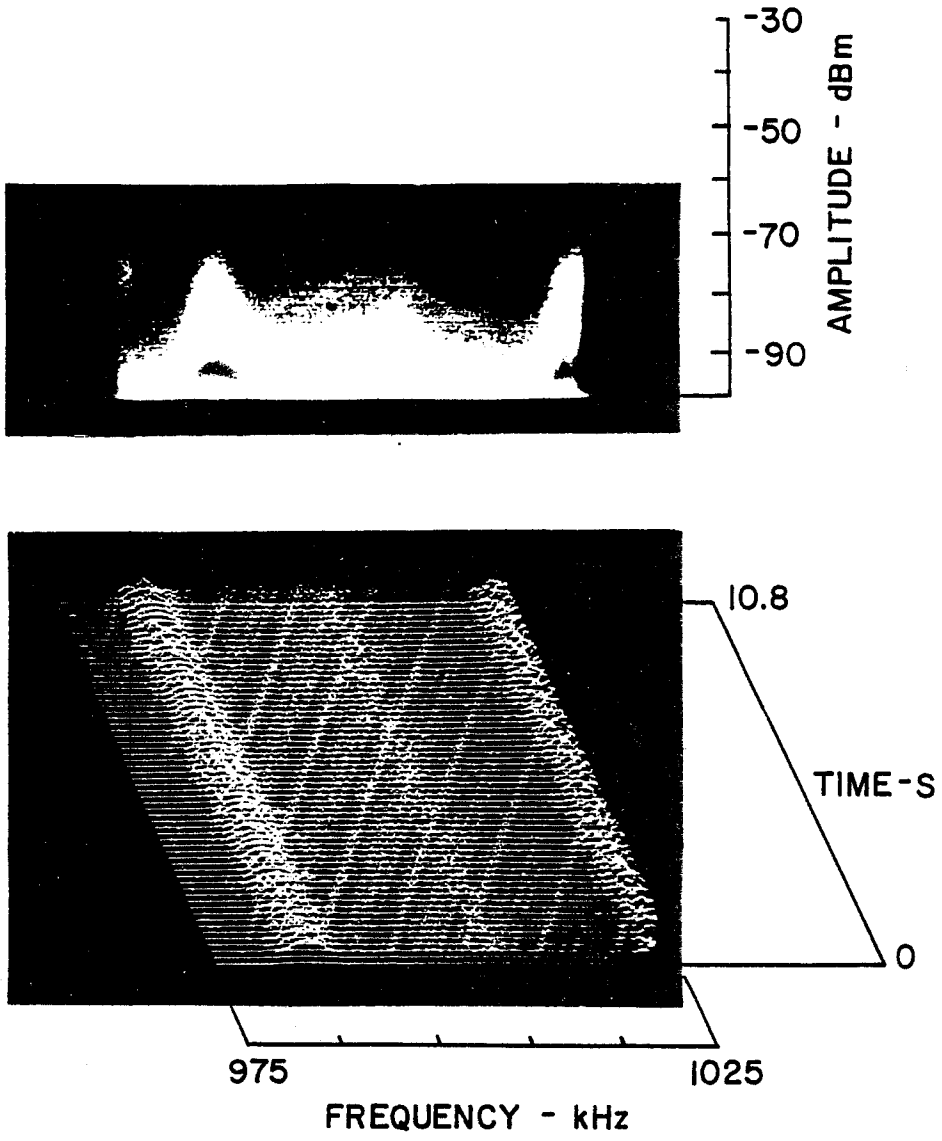

Figure 5 UTC Riser Pole Site, 6/27/78, 1149

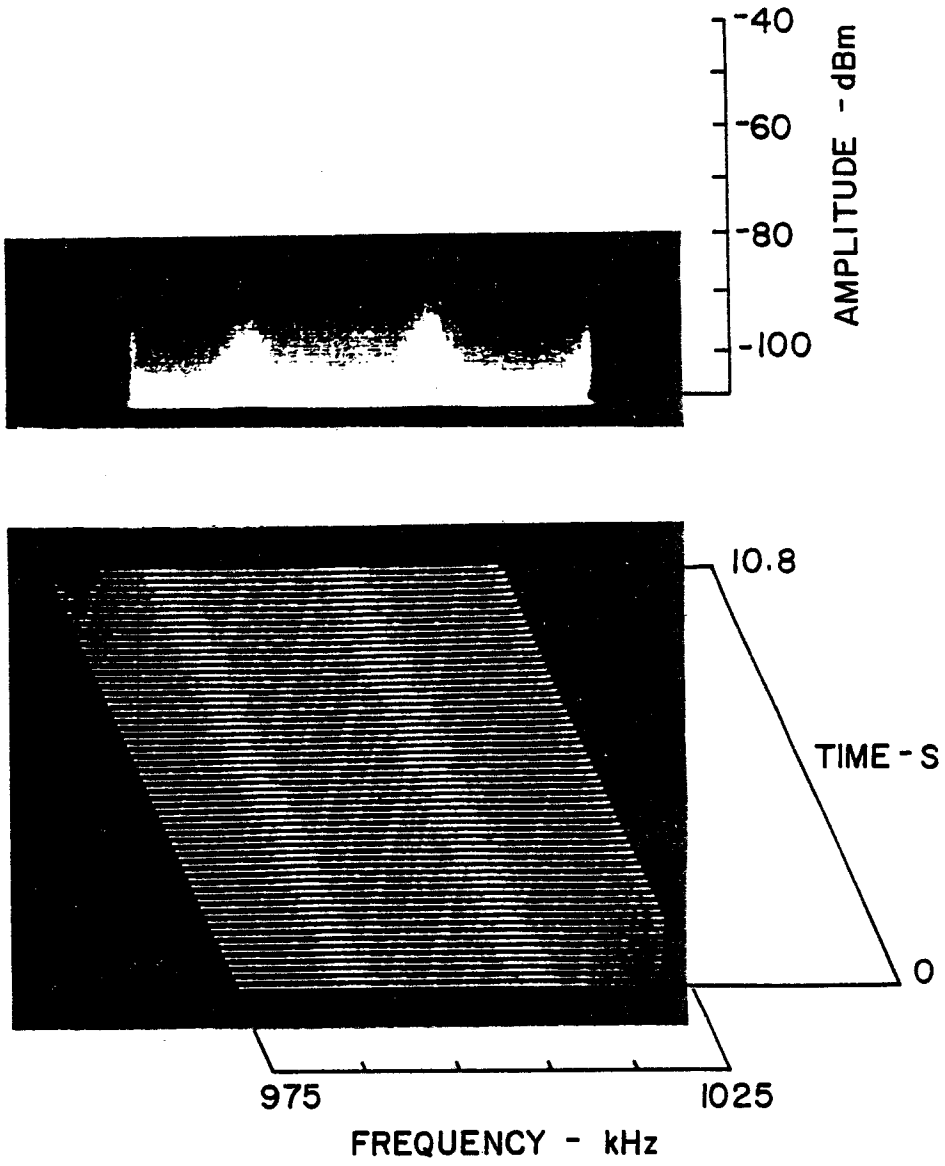

Figure 6 UTC Riser Pole Site, 6/27/78, 1157

3.3.3 Converter Measurements

Observations of noise with the converter on were started immediately after the completion of a reasonable sample of background noise. A very large increase in noise was immediately noted at the 25 to 75 kHz frequencies when the converter was turned on as shown in Figure 7. The measurement was made with the UTC Riser Pole capacitor bank on and the Spring Pond Park capacitor bank on.

The data in Figure 8 were taken with the UTC Riser Pole capacitor bank on, the Spring Pond Park capacitor bank off, and as the inverter was turned off. The three views show the same data with various display geometry variations to portray the primary properties of the noise before and after converter shutdown. The frequency and time scales on the lower view also apply to the middle view. Noise amplitude vs. frequency is shown in the upper view.

In Figure 8 the converter was operating from 10.8 seconds down to about 4 seconds on the time scale. From 4 seconds down to 0 seconds the converter was off, and background noise can be seen in the lower portion of the two bottom views.

The data in Figure 9 were taken with the converter on, the Spring Pond Park capacitor bank on, and as the UTC Riser Pole capacitor bank was switched from off to on. Significant changes in the spectral shape of the noise were caused by the capacitor bank switching at 6 seconds on the time axis. These changes were:

a. Converter-generated noise from 22 to 30 kHz was severely attenuated by the capacitor bank.

b. Converter-generated noise from 30 to 37 kHz was not affected.

c. Converter noise from 37 to above 40 kHz increased significantly in level.

The above-listed changes in the spectral properties of converter-generated noise suggested that the capacitor bank effectively bypassed the noise up to about 30 kHz. Above 37 kHz the capacitor bank appeared to behave as a peaking inductor which enhanced noise level at the 37 to above 40 kHz frequencies.

The data in Figure 10 were taken with the converter on, the Spring Pond Park capacitor bank on, and as the UTC Riser Pole capacitor bank was switched off. Converter-generated noise between 25 and 30 kHz was attenuated when the capacitor was in the circuit from 10.8 down to about 5 seconds on the time scale. At 5 to 0 seconds, the mid-band noise at 30 to 50 kHz decreased in level, noise at 25 to 30 kHz increased in level, and a small band of noise from 50 to 60 kHz remained unchanged. The frequency range in Figure 10 was somewhat larger than that of the previous figure (50 kHz wide in place of 20 kHz) which produced a somewhat different appearance between the two views, but the 25 to 40 kHz data common to both figures were very similar.

The data in Figure 11 were taken with the converter on, the Spring Pond Park capacitor bank in, and as the UTC Riser Pole capacitor bank was switched on. The test conditions were similar to that for Figure 10 except that the capacitor bank switched on in place of off. The converter-generated noise results were very similar to the previous example (except for the reversal of conditions between the top and bottom portions of the lower 3-axis views). In Figure 11 the scanning receiver timing permitted the observation of large transients as the capacitor bank was switched into the circuit. Switching transients exceeded the converter noise by about 30 dB at 30 kHz. Three separate transients were associated with capacitor bank switch closures on each phase of the distribution line.

The data in Figure 12 were taken with the measurement van located about 300' from the distribution line, the UTC Riser Pole capacitor bank on, the Spring Pond capacitor bank on, and as the converter was switched

on. Noise over the 10 to 110 kHz band was examined at the more distant location. Converter noise was noted over the 30 to 70 kHz band starting at 8 seconds on the time axis when the converter was turned on. The amplitude vs. frequency pattern in the upper view of Figure 12 showed strong peaks and nulls which implied resonance properties of the source/transmission line/radiation mechanism involved in the generation and radiation of the noise.

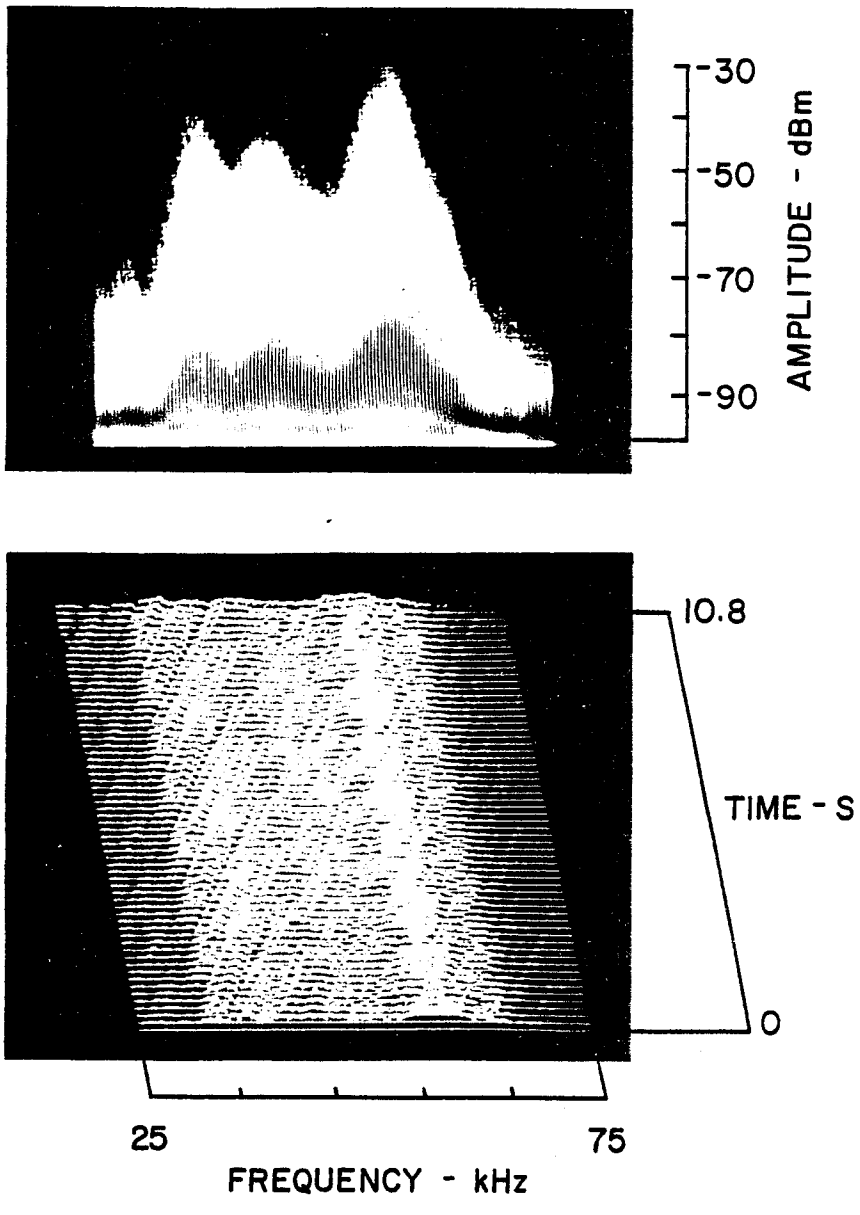

Figure 7 UTC Riser Pole Site, 6/27/78, 1126